Radiation acoustics

L. M. Lyamshev

N. N. Andreev Acoustical Institute of the Russian Academy of Sciences
(Submitted 3 December 1991)
Sov. Phys. Usp. **162**, 43–94 (April 1992)

A review is given of results of research on the excitation of sound in a condensed medium by penetrating radiation (beams of protons, electrons, photons, etc.) that is both modulated in intensity and pulsed. The thermoradiation (thermoelastic) mechanism is examined in detail when the volume density of the energy released in the medium is not great and no phase changes occur in it. Other mechanisms of radiation excitation of sound are also examined: formation of microshock waves, and the bubble, dynamic, striction and Cherenkov mechanisms. Some applications of radiation acoustics are discussed: radiation-acoustic microscopy and visualization, acoustic detection of superhigh-energy particles, a possible use of a neutrino beam for radiation-acoustic transillumination of the Earth.

1. INTRODUCTION

Modern acoustics is a wide field of science. Despite its considerable age (the ancient Greeks and Romans knew the foundations of architectural and musical acoustics), it continues to develop successfully and most extensively in boundary areas. Radiation acoustics, which is the subject of this review, is a striking example. It appeared at the interface of acoustics, high-energy physics, and nuclear and elementary particle physics. The basis of this field is the study of sound generation in a material by penetrating radiation and the application of radiation acoustic effects.

Radiation acoustics has drawn the attention of many researchers and specialists because the development of new radiation-acoustic technologies is connected with this field. These technologies are in use already or can find application in the near future in various fields of human activities of such different scale as microelectronics, geology and astronomy.

Many papers have been published on the topic of the various mechanisms of sound generation by penetrating radiation. The studies of thermoradiational (thermoelastic) mechanism of sound generation in liquids and isotropic solids can be considered to be the most advanced and to some extent completed. In this case the density of energy evolved in a medium due to absorption of penetrating radiation is not great and there are no phase transitions in a medium. An acoustic signal arises due to thermal expansion of a substance. An overwhelming majority of applications of radiation-acoustic effects is also connected with the thermoradiational mechanism.

We deliberately do not consider nonlinear acoustic effects caused by the action of powerful penetrating radiation beams on a substance assuming that this is the subject of a separate consideration due to its specific character. It was also not possible to include in the list of cited literature all papers considering radiation acoustics (even very interesting ones).

The review is based on the materials of invited lectures delivered by the author at the 1st French National Acoustic Conference (April 1990, Lyon), the International Congress on Ultrasonics (December 1990, Delhi, India) and the 9th All-Union Acoustic Conference (June 1991, Moscow, USSR).

2. WHAT IS RADIATION ACOUSTICS?

Radiation acoustics is a branch of acoustics developing at the interface of acoustics, nuclear physics and high-energy and elementary-particle physics. The study of sound excitation in a substance by penetrating radiation (proton, electron and neutral particle beams, x-rays and synchrotron radiation, γ-quanta, single high-energy particles, etc.) lies at its base. Sound excitation by laser radiation (photon beams) is of the same nature also.

The study of radiation-acoustic effects opens up new opportunities in the investigation of penetrating radiation itself (acoustical detection and radiation-acoustic dosimetry), in the investigation of the physical parameters of matter (radiation-acoustic microscopy), in the solution of nontraditional applied problems of nondestructive testing (radiation-acoustic flaw detection and visualization). New unique opportunities of targeted radiation-acoustic influencing of physical-mechanical and chemical parameters of a substance arise.

The research on radiation-acoustic effects was stimulated mainly by the progress of high-energy and elementary-particle physics. Elementary-particle physics has developed rapidly during the last decades. Beams of tremendous energy of hundreds and thousands gigaelectronvolts (GeV) have been obtained with the help of super-powerful accelerators. New generations of accelerators for energy of tens and hundreds teraelectronvolts (TeV) are under construction now. A great number of particles subjected sometimes to amazing transformations and interactions has been discovered with the help of accelerators. Quantum chromodynamics and unified theory of electromagnetic and weak interaction appeared and the state-of-the-art is now that physics is on the verge of creating the grand unification theory (GUT) of all the fundamental interactions—electromagnetic, strong (nuclear), weak and gravitational interactions. Experimentation at even greater energy is necessary for the solution of this problem. As the construction of the new generations of powerful accelerators opens up new vistas for elementary-particle physics studies in the range of higher and higher energy, the accelerators constructed initially for such research are used more and more widely in the research in physics of solids, biology, and medicine and in radiation-

 0038-5670/92/040276-27$03.00

acoustic studies. On the other hand, estimates show, for example, that it might be impossible even in the distant future to construct super-powerful accelerators for the energy required by physicists for the realization of the new ideas of GUT. Only "natural" accelerators existing in the bowels of galaxies are capable of generating particles, for example, neutrinos, with an energy up to 10^8 TeV and more, but huge detectors are needed to detect particles of such energy on the Earth. And in this case the acoustic detection methods can turn out to be justified economically (see Note 1 at the end of the article).

3. FROM THE OPTOACOUSTIC EFFECT TO THE RADIATION-ACOUSTIC EFFECT AND RADIATION ACOUSTICS

The beginning of radiation acoustics is connected in a broad sense with the discovery by A. Bell, W. Roentgen and J. Tyndall of the optoacoustic (photoacoustic) effect that is sound generation in a gas volume due to intermittent (modulated) light passage or, in other words, due to modulated optical radiation (modulated photon beam) interaction with a substance (gas).[1-3] At the same time A. Bell discussed the question of construction of a radiophone—"a device for producing sound by radiation of any kind."[2] Further studies of the optoacoustic effect served, as is known, as the basis for the development of optoacoustics (photoacoustics) including optoacoustic spectroscopy of gases and condensed media. A powerful stimulus for the development of this field in the last decades was the construction of lasers.

The first studies of radiation-acoustic effects have been conducted in the 50's and 60's. So, for example, in 1956 academician I. M. Lifshits, M. I. Kaganov and D. V. Tanatarov[4] considered sound radiation in a solid by a uniformly moving electron and showed that at an electron velocity greater than the sound velocity in a medium (see Note 1 at the end of the article), Cherenkov radiation of sound (phonons) takes place. The analogous problem was considered earlier (1953) by M. Buckingham.[5] In 1955 D. Glaser and D. Rahm published an article[6] in which they reported the possibility of recording passage of a particle in a bubble chamber by vibrations of the chamber walls caused by an acoustic signal generated by the formation of bubbles on a particle track. In 1957–59 G. A. Askaryan has considered radiation of ultrasonic and hypersonic waves by charged particles in dense media due to local heating and formation of cavities along particle tracks[7,8] (see Note 2 at the end of the article).

In 1963 R. White has investigated experimentally sound excitation by a low-energy electron beam in a solid.[9] Somewhat later (1967) R. Graham and R. Hutchison[10] have made measurements of mechanical oscillations in quartz crystals, sapphire, etc. on their being irradiated by electron beam pulses, and in 1969 B. Beron and R. Hofstadter observed mechanical oscillations arising in ceramic piezosensors under the action of relativistic electrons.[11] B. Beron and R. Hofstadter, as G. A. Askaryan[7,8] before them, supposed that not only electrons but also other "elementary" particles can generate mechanical oscillations due to their interaction with a substance. In the 70's, numerous studies of sound excitation in condensed media by electron and proton beams and by single particles were conducted in the USSR by I. A. Borshkovskiĭ, V. D. Volovik, I. I. Zalyubovskiĭ, A. I. Kalinichenko, V. T. Lazurik and others (see the book of Ref. 12 and references cited in it), and in the 80s—by L. M. Lyamshev and B. I. Chelnokov (see, for example, Refs. 13, 14).

The publications of many foreign researchers on possible applications of the radiation-acoustic effects date to the same period (see, for example, F. Perry *et al.* on the application of these effects to the dosimetry of pulsed beams of accelerated particles and to obtaining data on the depth distribution of irradiation dose in a target.[15]

Research on radiation-acoustic effects could hardly have drawn attention of the physicists in the last decades if it were not connected with the prospects of its practical applications. Scanning radiation-acoustic microscopy of condensed media,[16-22] acoustic detection of super-high-energy particles (the DUMAND Project—Deep Underwater Muon and Neutrino Detection),[23-28] research on the role of the radiation-acoustic mechanism in underwater noise generation in calm ocean,[29] and also the opportunities opening up for the application of new generations of proton and linear super-powerful accelerators to the production of super-high-energy neutrino beams (~ 10 TeV) and the applications of these beams in geoacoustics (neutrino geoacoustics, the GENIUS Project—Geological Exploration of Neutrino-Induced Underground Sound)[30,31] and in neutrino-acoustic ocean tomography[32] should be mentioned here in the first place.

4. MECHANISMS OF SOUND GENERATION BY PENETRATING RADIATION

A definite conception has been formed by now about the mechanisms of sound generation by penetrating radiation. They are connected usually with the physical phenomena (processes) resulting in the transformation of penetrating radiation energy into acoustic energy. They depend on the radiation type, on the target substance in which this radiation is absorbed, and on the energy release mode in the absorption area. The mechanisms of sound radiation by penetrating radiation are numerous and not equal in their efficiency.[33]

4.1. Thermoradiation mechanism

Heat release is one of the most universal physical phenomena taking place due to penetrating radiation absorption. Thermal energy can transform into sound wave energy in different ways. At moderate released energy densities when no phase changes occur in a substance the main contribution to the sound generation process is due to the thermal expansion of a region of the medium where the radiation is absorbed. This is the thermoradiation (thermoelastic) mechanism of sound generation. In this case the sound fields can be described within the framework of the linear theory which has been developed extensively, especially in recent years.[12-14]

The solutions of boundary-value problems for an inhomogeneous wave equation with the right-hand side containing the function describing the power density of thermal sound sources which are due to penetrating radiation absorption in a substance, are usually basic for the theoretical consideration. This equation for liquid media has the form

$$\Delta p - \frac{1}{c^2}\frac{\partial^2 p}{\partial t^2} = -\frac{\beta}{C_p}\frac{\partial Q}{\partial t}, \qquad (1)$$

or

$$\frac{\partial^2 p}{\partial t^2} - c^2 \Delta p = \Gamma \frac{\partial Q}{\partial t}, \tag{1'}$$

where p is the sound pressure, c is the sound velocity, β is the volume thermal expansion coefficient, C_p is the liquid specific heat, Q is the function characterizing the energy release (absorption) of penetrating radiation or the thermal sound sources power density and $\Gamma \equiv c^2\beta / C_p$ is the Grüneisen parameter.

In the case of an isotropic solid we have

$$\left(\Delta - \frac{1}{c_l^2}\frac{\partial^2}{\partial t^2}\right) \operatorname{div} \mathbf{u} = \frac{(3-4n^{-2})\alpha}{C_\varepsilon \rho} \int \Delta Q dt - \frac{\operatorname{div} \mathbf{F}}{c_l^2 \rho}, \tag{2}$$

$$\left(\Delta - \frac{1}{c_t^2}\frac{\partial^2}{\partial t^2}\right) \operatorname{curl} \mathbf{u} = \frac{\operatorname{curl} \mathbf{F}}{c_t^2 \rho}. \tag{3}$$

Here c_l and c_t are respectively the transverse and longitudinal wave velocities, $n = c_l/c_t$, $\mathbf{u}$ is the displacement vector of the solid, ρ is the density, α is the linear thermal expansion coefficient, C_ε is the specific heat of the solid and $\mathbf{F}$ is the external nonthermoelastic force applied to a unit volume of the solid (its nature will be explained further). $F \equiv 0$ if only the thermoradiation mechanism of sound generation is considered and, therefore, only thermal sound sources are taken into account.

One can see from the equations given above that the sound pressure amplitude is directly proportional to the value of the Grüneisen parameter Γ and depends on the energy release function Q (power density of the thermal sound sources).

The form of the function Q for various types of penetrating radiation is different. For electromagnetic radiation

$$Q(x_1, x_2, x_3, t) = \mu J(x_1, x_2, t) \exp(-\mu x_3), \tag{4}$$

where x_3 is the coordinate in the radiation beam direction, μ is the radiation absorption coefficient in the medium or the reciprocal of the mean free path of the radiation quanta in the medium. For example, $\mu = 0.17\ \text{cm}^{-1}$ for the light wavelength $\lambda_l = 1.06\ \mu\text{m}$ (radiation of a Nd-glass laser) and pure water and $\mu = 800\ \text{cm}^{-1}$ for CO_2-laser radiation ($\lambda_l = 10.6\ \mu\text{m}$) and pure water.

The formula (4) is true for different types of electromagnetic radiation: light, x-rays, synchrotron radiation, γ-quanta beams, etc., and also for relativistic electrons, the energy losses of which due to interaction with a substance are connected with radiation (radiation losses). In the last case this dependence is presented in the form:[34]

$$\frac{1}{E_e}\frac{\partial E_e}{\partial x_3} = -\frac{1}{x_0}; \tag{5}$$

here E_e is the incident electron kinetic energy and x_0 is the radiation length (mean free path of a relativistic electron in the medium). We note that the penetrating radiation intensity in a beam can be represented by the expression

$$J(x_1, x_2, t) = n_p(x_1, x_2, t) E_e, \tag{6}$$

where $n_p(x_1, x_2, t)$ is the particle (electron) density. We have for the function of energy release

$$Q(x_1, x_2, x_3, t) = -n_p(x_1, x_2, t)\frac{\partial E_e(x_3)}{\partial x_3}. \tag{7}$$

It can be seen easily from (5)–(7) that (4) is true for relativistic electrons if we set $x_0 = \mu^{-1}$.

The losses are determined by ionization if the electron energy is low (nonrelativistic), yet greater than the average excitation energy of an atom of the substance with which the electron beam interacts. It is known that the radiation losses increase with increasing energy E_e almost precisely linearly, while the losses in energy E_e due to ionization increase only logarithmically. Therefore, the radiation losses are dominant at large values of the energy E_e (at relativistic velocities) and ionization plays a more and more important role as the energy decreases until the ionization losses will equal the radiation losses at some critical energy $E_{e,cr}$.

For example, for water $E_{e,cr} = 100$ MeV and for lead $E_{e,cr} = 10$ MeV. In the case of electron energy greater than the critical one, energy losses are described (average values) by the exponential law corresponding to (5) and (4). Therefore a relativistic electron beam with an energy of 1 GeV will lose in water up to 90%, and in lead up to 99%, of its energy according to the exponential law (4) and only about 10% or 1% respectively will be due to ionization losses.

In the case of heavy charged particles, to which belong protons, nuclei of different atoms, and particles in general involved in strong interactions, the law (4) cannot be used. Heavy charged particles lose their energy in passing through a substance mainly because of inelastic collisions with bound electrons of atoms of the substance slowing them down. When a particle velocity becomes so small that the particle captures electrons, energy losses decrease. However, the particle deceleration continues until its energy becomes equal to the thermal energy of atoms of the medium. Therefore, for example, as a proton moves in a substance its losses will increase until it begins capturing electrons from atoms of the substance. After that the losses will decrease. There must be a maximum on the curve characterizing the dependence of the proton energy losses on its so called residual range. This fact is observed in reality. This maximum is called the Bragg peak[34] in nuclear physics.

If particles have a very high energy sufficient for production of numerous secondary particles (hadrons, pions, etc.) then nuclear-electron-photon cascades arise in a substance due to the absorption of penetrating radiation particles in the substance. We can consider the energy absorption in a cascade to be approximately exponential.

Slowing-down of neutral heavy particles in condensed media (the most important such particles are neutrons) is due to their direct collisions with the nuclei of atoms of the target substance. In these cases it is usually difficult to obtain universal analytical relationships and one has to be satisfied with specific calculations and empirical relationships based on experimental data. We note only that the energy losses of neutral heavy particles are significantly lower than the corresponding losses of charged heavy particles, and, therefore, their penetration depth in a substance is significantly greater than that of charged heavy particles.

Thus, the determination of the analytical form of the energy release function Q can be difficult in many cases. Therefore, the exponential law of absorption of penetrating radiation in a substance is often adopted in considering the concrete problems of thermoradiation generation of sound, and the radial intensity distribution in a beam is assumed to

be Gaussian. This allows one to obtain results in a final form. Detailed consideration shows that the basic conclusions of the theory remain valid in the majority of cases also for other radiation types, the absorption of which in a substance is not governed by the exponential law.[14]

4.1.1. Sound generation by harmonically modulated penetrating radiation

Let us consider the special features of the thermoradiation generation of sound in a condensed medium. We shall limit ourselves to the case of isotropic liquid and solid media.

Sound field in the far wave zone of a thermoradiation sound source (TRSS) in a liquid arising due to the action on its surface of penetrating radiation with intensity varying harmonically with the sound frequency f and under the condition that the absorption of radiation quanta in a liquid is governed by the exponential law and in the case of the Gaussian distribution of radiation intensity, is described by the expression

$$p(r) = -\frac{A\omega m\beta W}{2\pi C_p}\frac{\exp(ikr)}{r}\frac{\mu k\cos\theta}{\mu^2 + k^2\cos^2\theta}\exp\left(-\frac{k^2a^2}{4}\sin^2\theta\right); \tag{8}$$

here $p(r)$ is the sound pressure, $k = \omega/c$, m is the radiation intensity modulation index, r is the distance to the observation point, θ is the angle between the direction to the observation point and the normal to the liquid surface (penetrating radiation beam direction of incidence on the liquid surface), W is the penetrating radiation power ($W = \pi a^2 J_0$), a is the beam radius, J_0 is the radiation intensity, A is the transparency coefficient of a liquid surface for penetrating radiation. The factor $\exp(-i\omega t)$ is omitted as usual.

The expression (8) describes also the normal stress tensor σ_{RR} (longitudinal waves) of the analogous TRSS in an isotropic solid (elastic half-space) with a precision up to a sign ($\sigma_{RR} = -p$) and the relationship for the volume β and the linear α coefficients of thermal expansion $\beta = 3\alpha$.

It can be seen that the sound pressure amplitude in the far wave field of a harmonical TRSS increases linearly with the power growth of penetrating radiation $p \sim W$; TRSS directivity pattern depends on the wave parameters ka and $k\mu^{-1}$. If $ka \ll 1$ and $k\mu^{-1} \ll 1$ dipole radiation of sound is observed. At $ka \ll 1$ and $k\mu^{-1} \gg 1$ TRSS has the form of a rod elongated along the beam direction and the sound propagates mainly along the free surface of the liquid, and at $ka \gg 1$ and $k\mu^{-1} \ll 1$ TRSS takes on the form of a disk and the sound is emitted mainly in the direction of the penetrating radiation beam in the liquid; i.e. along the normal to the liquid surface. The factor $A\omega\beta mW/2\pi C_p$ in (8) can be written in the form $(A\omega mW/2\pi c^2)\Gamma$ where $\Gamma = \beta c^2/C_p$ is the Grüneisen parameter. It follows from this that the sound pressure amplitude is directly proportional to the value of the Grüneisen parameter of the medium.

Sound pressure amplitude depends on the parameter μ, i.e. on the mean free path of the radiation quanta in the medium or on the radiation length (in the case of ultra-relativistic electrons). The condition $k \approx \mu$ can be shown to be the optimal condition for sound excitation in a liquid. Meanwhile, the parameter μ depends on the parameters of the medium, the type of radiation and the energy of the quanta (the energy of the particles). Therefore, one can optimally excite sound waves of prescribed wavelength by selecting radiation type and particle energy.

An important characteristic is the so-called radiation-acoustic conversion coefficient. When the penetrating radiation beam radius is large compared with the sound wavelength $ka \gg 1$, and at $k \approx \mu$, the following expression holds for the radiation-acoustic conversion coefficient

$$\eta = \frac{W_{ak}}{W} = \frac{c}{\rho}\frac{mA\beta}{4C_p}J_0. \tag{9}$$

For example, if we take for water $\beta = 3\cdot 10^{-4}$ grad^{-1} and $A = 1$ then we shall have at $k = \mu$

$$\eta_{\max} = 5\cdot 10^{-12}J_0, \text{ where } J_0 \text{ is in W/cm}^2$$

The threshold value of J_0, at which there are as yet no nonlinear effects connected with phase transitions, depends on the value of the volume density of energy released in the medium. At a given radiation power W the value of the intensity will depend on the beam radius and the mean free path of the penetrating radiation particles in the medium. For example, for water and CO_2-laser radiation $J_{e,thr} \leqslant 10^6$W/cm^2. Therefore, the conversion efficiency cannot be higher than $\eta \leqslant 10^{-5}$.

The following expression holds for sound pressure in the near wave zone of TRSS

$$p(r) = i\frac{Am\beta c}{C_p}\frac{\mu k}{\mu^2 + k^2}J_0\exp\left(-\frac{x^2 + y^2}{a^2}\right). \tag{10}$$

An important consequence follows from (10): the sound pressure amplitude in the near wave field varies in direct proportion to the penetrating radiation intensity and not to the power as in the TRSS far wave field.

We shall return to these conclusions in considering the experimental data.

4.1.2. Sound excitation by radiation pulses

Sound excitation by radiation pulses is of interest for two reasons at least. First, the majority of penetrating radiation sources operates in a pulsed regime, as a rule. Second, tremendous penetrating radiation power (intensity) and, therefore, high efficiency of radiation-acoustic conversion can be realized in a pulsed regime.

Sound excitation by penetrating radiation pulses and especially by laser pulses was studied by many researchers (see, for example, Refs. 14, 35–37). We shall cite the most characteristic results.

The expression for sound pressure in a liquid in the far wave zone of TRSS created by a penetrating radiation pulse of arbitrary form acting on the liquid surface, has the form[37]

$$p(r, t) = \frac{1}{2\pi}\int_{-\infty}^{\infty} p_\omega(r)\exp(i\omega t)\mathrm{d}t, \tag{11}$$

$$p_\omega(r) = -\frac{A\beta W}{2\pi C_p}\frac{\exp(ikr)}{r}\frac{\omega^2\tau_\mu}{1 + \omega^2\tau_\mu^2}\exp\left(-\frac{\omega^2\tau_a^2}{4}\right)F(\omega). \tag{12}$$

We have after substitution of (12) into (11)

$$p(r, t) = -\frac{A\beta W}{4\pi^2 C_p r \tau_\mu^2}\int_{-\infty}^{\infty}\exp\left(-\frac{k^2 s^2}{4}\right)\frac{k^2}{1+k^2}\exp(ik\gamma)F\left(\frac{k}{\tau_\mu}\right)dk; \quad (13)$$

here

$$k = \omega\tau_\mu, \quad \gamma = \frac{r}{c} - t, \quad s = \frac{\tau_a}{\tau_\mu},$$

$$\tau_a = \frac{a\sin\theta}{c}, \quad \tau_\mu = \frac{\cos\theta}{\mu c}, \quad r = (x^2 + y^2 + z^2)^{1/2},$$

$$F\left(\frac{k}{\tau_\mu}\right) = F(\omega) = \int_{-\infty}^{\infty} f(t)\exp(i\omega t)d\omega,$$

where $f(t)$ is the function describing the radiation pulse envelope.

It follows from (13), for example, that for $\tau \gg \tau_a$ and $\tau \gg \tau_\mu$

$$p(r, t) \approx \frac{A\beta W}{4\pi^2 C_p r}\tau_\mu f'\left(t - \frac{r}{c}\right), \quad (14)$$

while for $\tau \gg \tau_a$ and $\tau \ll \tau_\mu$

$$p(r, t) = \frac{A\beta W}{4\pi^2 C_p r}\left\{f\left(t - \frac{r}{c}\right) - \pi\frac{\sigma}{\tau_\mu}\exp\left[-\left(t - \frac{r}{c}\right)\right]\right\}, \quad (15)$$

where

$$\sigma = \int_{-\infty}^{\infty} f(t)dt$$

is the "area" of the radiation pulse. Three important consequences follow from (14) and (15). First, in the case of "long" radiation pulses $\tau \gg \tau_a, \tau_\mu$ the acoustic signal amplitude increases linearly with increasing radiation pulse power, and, secondly, the acoustic signal form is determined practically completely by the second derivative of the radiation pulse envelope $f''(t)$. Third, for pulses short compared with the sound waves propagation time along the generatrix of the TRSS in the beam propagation direction in the liquid $\tau \ll \tau_\mu, \tau \gg \tau_a$ the sound signal represents a rarefaction pulse reproducing the envelope of the "overturned" radiation pulse with a positive addition proportional to the small parameter $\pi(\sigma/\tau_\mu)$. We note that the presence of this "positive splash" is of a fundamental character, and must not be associated with equipment distortions as it might seem to an experimenter.

Let us consider now the characteristic case of short radiation pulses but wide penetrating radiation beams. We have from (13)

$$p(r,t) = -\frac{A\beta\mathscr{E}}{16\pi C_p \tau_\mu^2 r}\left\{\frac{4}{\sqrt{\pi}s}\exp\left(-\frac{\gamma^2}{s^2}\right) - \exp\frac{s^2}{4} \times\left[\exp(-\gamma)\mathrm{Erfc}\left(\frac{s}{2} - \frac{\gamma}{s}\right) + (\exp\gamma)\,\mathrm{Erfc}\left(\frac{s}{2} + \frac{\gamma}{s}\right)\right]\right\}, \quad (16)$$

where $\mathscr{E}$ is the energy in the radiation pulse and

$$\mathrm{Erfc}(z) = \frac{2}{\pi}\int_z^{\infty}\exp(-t^2)dt$$

is the auxiliary function of errors;

$$\mathscr{E} = \pi a^2 J_0 \sigma, \quad \sigma = \int_{-\infty}^{\infty} f(t)dt.$$

For $s \gg 1$ that corresponds to TRSS in the form of a wide disc and observation at angles θ which are not too small, we have

$$p(r, t) \approx -\frac{A\beta\mathscr{E}}{2\pi^{3/2}C_p\tau_\mu^2 s^3 r}\left\{\frac{2[t - (r/c)]}{\tau_a^2} - 1\right\} \times \exp\left\{-\frac{[t - (r/c)]^2}{\tau_a^2}\right\}. \quad (17)$$

If $s \ll 1$, that corresponds to TRSS in the form of a long cylinder and observation at small angles θ, we have

$$p(r, t) \approx -\frac{A\beta\mathscr{E}}{8\pi C_p r\tau_\mu^2 s}\left\{\frac{2}{\sqrt{\pi}}\exp\left[-\frac{(t - (t/c)^2}{\tau_a^2}\right] - s\exp\left[-\frac{|t - (r/c)|}{\tau_\mu}\right]\right\}. \quad (18)$$

Two important consequences follow from (15)–(18). First, in the case of short radiation pulses the acoustic signal amplitude varies in direct proportion to the radiation pulse energy (and not to its power!), and, secondly, the acoustic signal always has a universal form and does not depend on the form of the radiation pulse (envelope).

These conclusions are completely valid also in the case of sound generation by laser pulses in solids. The formulas (12)–(16) with some unimportant corrections are suitable for the description of acoustic signals from longitudinal (normal stresses σ_{RR}) and shear (shear stresses $\sigma_{R\theta}$) waves.[14]

4.1.3. Moving thermoradiation sound sources

A moving thermoradiation source of sound arises as a result of movement of a penetrating radiation beam over the surface of a condensed medium. Theoretical studies of moving TRSS were carried out in particular in Refs. 38–40.

Let us consider as a characteristic example the special features of sound generation in a liquid by a penetrating radiation beam moving upon its surface, the beam intensity being modulated by a pulse of arbitrary form. There are practically no limitations imposed on the beam movement velocity upon the liquid surface and on the form of its trajectory. It is presumed only that the beam movement trajectory is located in a finite area of the liquid surface, and the sound field is considered in the far wave zone relative to the dimensions of this area (the dimensions of the moving TRSS).

The equation for a sound pressure spectrum in the liquid p_ω generated by a moving penetrating radiation beam takes on the form (after simple transformations (1) and (4))

$$\Delta p_\omega + k_0^2 p_\omega = \frac{A\mu J_0\beta}{C_p}\exp(-\mu z)\int_{-\infty}^{\infty}\exp\left[i\omega t - \frac{(x - x_0(t))^2}{a^2} - \frac{(y - y_0(t))^2}{a^2}\right] \times\{f'(t) + 2\frac{f(t)}{a^2}(xx_0'(t) - x_0(t)x_0'(t) + yy_0'(t) - y_0(t)y_0'(t))\}dt. \quad (19)$$

where $x_0(t)$, $y_0(t)$ are the coordinates of the radiation spot movement over the liquid surface, k_0 is the complex wave number of sound, $f'(t)$, $x_0'(t)$, $y_0'(t)$ are respectively the derivatives of the functions $f(t)$, $x_0(t)$, $y_0(t)$.

We have from (19) for the wave zone

$$p_\omega = \frac{\beta}{C_p} AJ_0 a^2 \frac{\exp(ik_0 r_0)}{r_0} \frac{\omega^2 \tau_\mu}{1+\omega^2\tau_\mu^2} \times \exp\left(-\frac{1}{4}\omega^2\tau_a^2 - q(\omega)r_0\right)\tilde{F}(\omega), \tag{20}$$

where

$$\tilde{F}(\omega) = \int_{-\infty}^{\infty} f(t)\exp[i\omega t + ik_0 \sin\theta\cdot(x_0(t)\cos\varphi + y_0(t)\sin\varphi)]\,dt. \tag{21}$$

$\tau_\mu = (\cos\theta)/\mu c$, $\tau_a = (a\ \sin\theta)/c$, c is the sound velocity, θ is the angle between the z-axis and the position vector of the observation point r_0, φ is the angle between the x-axis and the projection of r_0 on the (x,y) plane, $q(\omega) = \mathrm{Im}k_0$ is the sound attenuation coefficient in a liquid, $k = \mathrm{Re}\,k_0$.

If we compare (20) with the analogous expression for the sound pressure spectrum of a stationary pulsed radiation-acoustic source (12) then we shall see that (12) and (20) differ only by the fact that in (20) the laser pulse spectral density $F(\omega)$ has been replaced by the function $\tilde{F}(\omega)$. This function is independent not only of the form and duration of the laser pulse but also of the characteristics of the laser spot movement upon the liquid surface.

The expression (20) was obtained on the basis of fairly broad assumptions. It follows from this expression that in this general case the sound pressure spectrum in a liquid is determined on the one hand by the geometrical parameters of the region of absorption of the penetrating radiation (as in the case of a stationary beam), and on the other hand—by a function dependent on the radiation pulse spectrum and on the parameters of the movement of the penetrating radiation beam.

The analytical expression (20) obtained for a sound field spectrum in a liquid appears to be very convenient for the consideration of various special cases of sound emission by a moving pulsed TRSS. Let us consider only one of them here.

Let a radiation spot move uniformly and rectilinearly with the velocity v along the x-axis, i.e. $x_0(t) = vt$, $y_0(t) = 0$. The function $\tilde{F}(\omega)$ is expressed in this case in terms of the radiation pulse spectrum in a simple way

$$\tilde{F}(\omega) = F((1-\tilde{\beta})\omega). \tag{22}$$

It follows from (20) and (22) that sound generation by a pulsed TRSS moving uniformly and rectilinearly occurs in the same way as in the case of a stationary, but $|1-\tilde{\beta}|$-times "compressed," radiation pulse described by the function $f[t(1-\tilde{\beta})/|1-\tilde{\beta}|]$ and its effective duration is $|1-\tilde{\beta}|\tau$ (here τ is the duration of a penetrating radiation pulse). We note that if $1-\tilde{\beta}<0$ then the "effective" pulse $f[t(1-\beta)]/|1-\tilde{\beta}|$ will be not only compressed but also inverted in time relative to the radiation pulse. This is connected with the fact that at the supersonic velocity of a radiation-acoustic source movement the distortions created later will arrive at the observation point earlier.

Thus, practically all the results and the discussion given above in Sec. 4.1.2, can be applied directly to the case of a moving pulsed TRSS if we consider the effective radiation pulse $f[t(1-\tilde{\beta})]/|1-\tilde{\beta}|$ with the duration $|1-\tilde{\beta}|\tau$.

We shall not consider further the details given already in Sec. 4.1.2. We shall consider here only the special features of sound radiation in the Cherenkov direction in the case of TRSS supersonic motion. The Cherenkov direction is determined by the equation

$$(V/c)\sin\theta\cdot\cos\varphi = 1.$$

If this condition is satisfied, sound distortions from different points of the TRSS are added synchronously, and, as follows from (22), the function $\tilde{F}(\omega)$ takes on a particularly simple form:

$$\tilde{F}(\omega) = F(0) = \int_{-\infty}^{\infty} f(t)\,dt = \sigma,$$

i.e. it does not depend on frequency and is equal to the "area" of the radiation pulse σ. Substituting $\tilde{F}(\omega)$ into (20) and evaluating the inverse Fourier transform we obtain the expression describing the sound field in the Cherenkov direction:

$$p(r,t) = -\frac{A\beta\mathcal{E}}{8\pi C_p r_0 \tau_\mu^2}\left\{\frac{4}{\sqrt{\pi}s}\exp\left(-\frac{\gamma}{s^2}\right) - \exp\frac{s^2}{4} \times\left[\exp(-\gamma)\,\mathrm{Erfc}\left(\frac{s}{2}-\frac{\gamma}{s}\right) + (\exp\gamma)\,\mathrm{Erfc}\left(\frac{s}{2}+\frac{\gamma}{s}\right)\right]\right\}, \tag{23}$$

where $\gamma = (r_0/c - t)/\tau_\mu$, $s = (\tau_a + 4cr_0)^{1/2}/\tau_\mu$, and $\mathrm{Erfc}(z)$ is the auxiliary error function. It is taken here for simplification that $q(\omega) = C\omega^2$ where C is some dimensional constant. We note that the expression (23) coincides with the formula (16) which describes sound generation by a very short radiation pulse, i.e. by a stationary pulsed TRSS.

It follows from (23) that the sound signal form in the Cherenkov direction does not depend on the form and duration of the radiation pulse, and the acoustic signal amplitude increases linearly with the increase in the radiation pulse energy. This theoretical conclusion will be compared with experimental data later.

4.1.4. Generation of sound by a high-energy particle

The theoretical analysis of sound generation by single particles is given in Refs. 14, 24–27 for different model situations: in a boundless space, in a solid half-space (volume waves), on the surface of a solid (the Rayleigh wave) and in a waveguide. Super-high-energy particles forming cascade showers due to their absorption in a substance were considered. Some results concerning sound generation by a high-energy particle in a boundless space will be given below.

The formation of the question of sound generation by single high-energy particles in a boundless space, i.e. when the distances from the sound generation area to free boundaries of the solid are large and sound waves reflected from boundaries can be ignored, is expedient only for high-energy neutrinos and muons of large penetrating capability which

can form nuclear-electromagnetic cascades deep in a solid.

Let us consider the case of a homogeneous and isotropic solid space taking into account that the result for a liquid space can be obtained readily as a particular case.

The initial equations are (2) and (3). It is assumed that the dynamic force is $\tilde{F} \equiv 0$ due to its insignificant role. We take the dependence of the energy release function $Q(t)$ on time in the form of a delta-function as the energy release time is much shorter than other characteristic times. The spatial dependence of the function $Q(r,t)$ we approximate by the expression[14]

$$Q(x,y,z) = \frac{\mu \mathscr{E}}{\pi a^2} \exp\left(-\frac{x^2+y^2}{a^2}\right) \exp(-\mu z)\Theta(z),$$

where $\mathscr{E}$ is the cascade energy, μ^{-1} is the effective cascade length, a is the effective cascade radius, and Θ is the Heaviside function. The origin of coordinates is chosen at the point of the cascade formation in this case, and the z-axis is directed along the cascade axis in the direction of its development. Such an approximation for the energy release function $Q(r,t)$ in spite of being rough, allows us nevertheless to investigate the main fundamental features of the sound field generated by a particle (see Note 3).

The expression for the normal component of the stress tensor in a sound field (longitudinal waves) in a boundless solid elastic medium has the form

$$\sigma_{RR} = -\frac{(3-4n^{-2})\alpha \mathscr{E}}{8\pi C_e R \tau_\mu^2} \left(\exp\frac{\tau_a^2}{4\tau_\mu^2}\right) \times \exp\left(-\frac{R-c_l t}{c_l \tau_\mu}\right) \operatorname{Erfc}\left(\frac{\tau_a}{2\tau_\mu} - \frac{R-c_l t}{c_l \tau_\mu}\right). \quad (24)$$

The near sound field of longitudinal waves in the observation direction perpendicular to the cascade axis is described by the expression

$$\sigma_{RR} = -\frac{(3-4n^{-2})\alpha}{4\pi C_e} \mu \mathscr{E} \left(\frac{c_l}{\pi R}\right)^{1/2} \int_{-\infty}^{\infty} \omega^{1/2} \exp\left(-\frac{\omega^2 a^2}{4c_l^2}\right) \times \cos\left[\frac{\pi}{4} - \omega\left(\frac{R}{c_l} - t\right)\right] d\omega. \quad (25)$$

The parameters of a cascade created by a single high-energy particle will be approximately equal for different liquid or solid media if the densities of these media and the charges of their component elements are close. So, if we assume that the parameters of a cascade from a neutrino with an energy of the order of $\mathscr{E} = 10^{15}$ eV in water are $\mu^{-1} = 4$ m, $a = 2$ cm, then an estimate of the effective sound pressure (in Pa) in the near wave zone according to the expression (25) is determined as follows ($f = 30$ kHz):

$$p_{\text{eff}} \approx 0.1(\mathscr{E}/\mathscr{E}_0) R^{-1/2}; \quad (26)$$

here and subsequently R is the distance (in meters), $\mathscr{E}_0 = 10^{16}$ eV. The formula (26) corresponds to the analogous expression for the sound signal level estimate in the far wave zone which is given in Ref. 41. If, for example, we take antarctic ice as the medium in which a cascade forms due to high-energy neutrino absorption in it, then the cascade parameters in it will be approximately the same as in water. In this case, if we take the numerical values of c_l, n, α corresponding to the ambient temperature $T = -20$ °C (Ref. 42) then the estimate of the effective sound pressure in the near wave zone is given (according to (25)) by the following relation ($f \approx 90$ kHz):

$$p_{\text{eff}} \approx (\mathscr{E}/\mathscr{E}_0) R^{-1/2}. \quad (27)$$

According to (26) and (27), the effective sound pressure in ice is approximately ten times larger than the effective sound pressure in water if other conditions are the same. This difference is due to the fact that the Grüneisen parameter for ice is approximately ten times larger than that for water.

For the far sound field with $\tau_a \gg \tau_\mu$, i.e. at observation direction practically perpendicular to the cascade axis, we have the following expression for longitudinal waves:

$$\sigma_{RR} = -\frac{3-4n^{-2}}{C_e} \frac{\mathscr{E}}{2\pi^{3/2}\tau_a^2} \frac{1}{R} \frac{R-c_l t}{c_l \tau_\mu} \exp\left[-\frac{(R-c_l t)^2}{c_l^2 \tau_a^2}\right]. \quad (28)$$

Correspondingly, the estimate for the effective sound pressure (in Pa) in ice under the conditions considered above, is

$$p_{\text{eff}} \approx 0.1(\mathscr{E}/\mathscr{E}_0) R^{-1}. \quad (29)$$

The analogous estimate for the effective sound pressure in water will be approximately ten times lower just as in the case of the near wave field. The boundary between the near and far sound fields for the cascade parameters given above and the effective frequency $f = 30$ kHz in water and $f = 90$ kHz in ice is approximately at the distance $R \approx 100$ m. The sound pressure in ice for the observation direction perpendicular to the cascade axis at the distance $R = 100$ m is approximately equal to $p_{\text{eff}} \approx 10^{-3}$ Pa and the sound pressure in water is 10^{-4} Pa (for particles with an energy of the order of $\mathscr{E} = 10^{16}$ eV).

4.1.5. Experimental study of thermoradiation generation of sound. Laser thermo-optical excitation of sound

Let us consider now the results of experimental investigation of thermoradiation sound generation in liquids and solids. We shall begin with some most characteristic results of experimental research of thermo-optical sound excitation.

Let us give the numerical estimates of sound pressure in water when its surface is acted upon by laser radiation with modulated intensity. We shall use the formula (8) and known values of parameters at the temperature $T = 18$ °C. We assume that the sound is generated by a modulated (intrapulse modulation) millisecond pulse of a neodymium laser with the energy $\mathscr{E} = 1.5$ kJ and duration $\tau = 1$ ms; the laser beam radius is $a = 2.5$ cm. The intrapulse light intensity modulation is 100% efficient ($m = 1$) and the optimal sound generation condition is satisfied (this corresponds to the modulation frequency $f = 100$ kHz). Water can be dyed in the absorption region to provide the given value of $k \approx \mu$. In this case according to (8) the sound pressure amplitude is equal to $p = 500$ Pa at a distance $R = 10$ m and in the direction $\theta = 0$. The half-width of the directivity pattern is $\Delta\theta = 0.2$ rad.

We give an estimate of a sound amplitude excited by a neodymium laser $\lambda_l = 1.06\ \mu$ with the parameters given above but in clear water $\mu = 0.17\ \text{cm}^{-1}$. If the sound frequency is 100 kHz, $k = 4\ \text{cm}^{-1}$ and the light beam radius is $a = 0.5$ cm then the amplitude of a sound wave in the direction of the TRSS directivity pattern maximum at an angle of approximately $\mu/k \approx 4.2 \cdot 10^{-2}$ rad to water surface is equal to $p = 90$ Pa at a distance $R = 10$ m.

It is accepted usually to characterize sound source efficiency by the value of the sound pressure normalized to a distance of 1 m. Then we have for the numerical estimates $p_1 = 5\ \text{kPa}\cdot\text{m}$ and $p_2 = 0.9\ \text{kPa}\cdot\text{m}$ respectively. The threshold value of sound pressure is frequently taken to be equal to $p_{\text{thr}} = 10^{-6}$ Pa. One can see from a comparison of p_1, p_2 and p_{thr} that sound oscillations in the case of thermo-optical excitation can attain considerable amplitudes. And this is despite the fact that the efficiency of laser thermo-optical conversion is very small. It is equal to $\eta \approx 10^{-5}$ in the case under consideration.

Let us consider the experimental results. Numerous experiments on laser excitation of sound in liquids and in solids were conducted under laboratory conditions and in water—also in natural conditions (see, for example, Ref. 43). The authors of Ref. 43 have conducted an investigation of laser sound generation in a lake. A neodymium laser ($\lambda_l = 1.06\ \mu$) was used which operated in a pulsed mode with intrapulse modulation of laser radiation intensity. The modulation frequency was chosen in such a way that the quasimonochromatic sound generation regime in water took place, i.e. the laser pulse duration was $\tau = 1$ ms and the modulation frequency was $f \simeq 20$–50 kHz. The sound pressure measurements were conducted at distances of 10.3 and 16.8 m from the TRSS.

The experimental data[43] agree satisfactorily with the conclusions of the theory of thermoradiation generation of sound. It follows from the theory that the sound pressure amplitude in the TRSS far wave zone increases linearly with penetrating radiation (laser radiation) power. This fact is confirmed experimentally. The theoretical dependence (solid line) and experimental data[43] (dots) are shown in Fig. 1a. The vertical axis represents the sound pressure level in decibels. Pressure values are reduced to the distance of 1 m and normalized relative to the pressure of 10^{-6} Pa. Fig. 1b shows theoretical and experimental[43] results characterizing the angle dependence of the sound field. The laser pulse duration was $\tau = 1$ ms as above, but the modulation frequency was $f = 50$ kHz and the distance at which the measurements have been conducted was 16.8 m. The light absorption coefficient in water was $\mu = 15.7\ \text{m}^{-1}$.

Numerous experiments on sound excitation in condensed media by laser pulses were conducted. Convincing correlation of experimental and theoretical data was obtained. We shall give only one of the characteristic examples confirming the theoretical conclusion concerning the universal form of sound pulses excited by "long" and "short" radiation (laser) pulses.

The authors of one of the first experimental investigations[44] in which the special features of acoustic signals excited in a liquid by laser pulses were studied, observed the acoustic pulse form alteration depending on the light absorption coefficient of a liquid, on the optical spot dimensions on its surface, and on the power and duration of a laser pulse. The alterations of the acoustic signal amplitude form observed by them did not agree with the theoretical one-dimensional model available at that time.[35,36] They associated this disagreement of the obtained experimental data and the theory with nonlinear effects which manifested themselves, from their point of view. In fact, the observed form alterations not only can be explained but serve as a convincing confirmation of the theory of thermoradiational (thermo-optical) sound excitation by laser pulses.[37,45] Fig. 2 shows sound pulses predicted by the theory on the assumption that a laser pulse has a rectangular form,[45] and also the pulses recorded in the experiment.[44] Both the calculations and the experiment illustrate both characteristic cases of sound signal excitation by "long" and "short" laser pulses and the fact that the sound signal form is universal.

It follows from the theory, as mentioned before, that in the case of "short" radiation pulses the sound signal amplitude increases linearly with increasing radiation (laser) pulse energy. Experimental data on sound excitation by laser pulses reliably confirm this theoretical conclusion. So, for example, the authors of Ref. 46 investigated the dependence of acoustic pulse amplitudes of longitudinal and shear waves on the energy of "short" laser pulses. It has been established that acoustic signal amplitudes increase linearly with increasing laser pulse energy (Fig. 3).

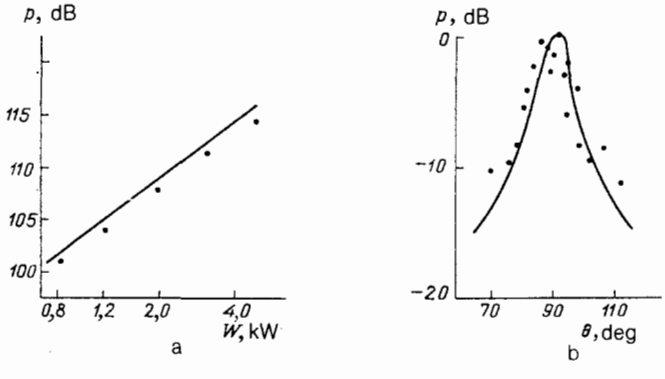

FIG. 1. a—The dependence of the sound pressure amplitude on the axis of a laser-acoustic sound source in water on the power of laser radiation.[42] b—The dependence of the sound pressure amplitude on the observation angle in the far wave field of a laser-acoustic sound source in water.[43]

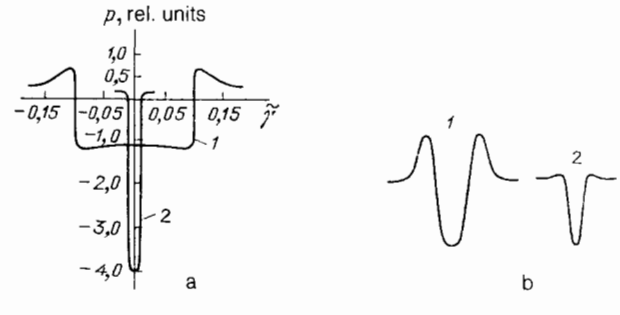

FIG. 2. a—Relative levels of sound pressure in water under the condition $s \ll 1$. *1*—$\tau = 13\ \mu$s, $\mu = 5\ \text{cm}^{-1}$, *2*—$\tau = 0.05\ \mu$s, $\mu = 1\ \text{cm}^{-1}$. b—Sound pulses registered experimentally by the authors of Ref. 44 during observation in the propagation direction of a laser beam. *1*—$\mu = 10^3\ \text{cm}^{-1}$, *2*—$\mu = 5\ \text{cm}^{-1}$; $\tau = 0.05\ \mu$s.

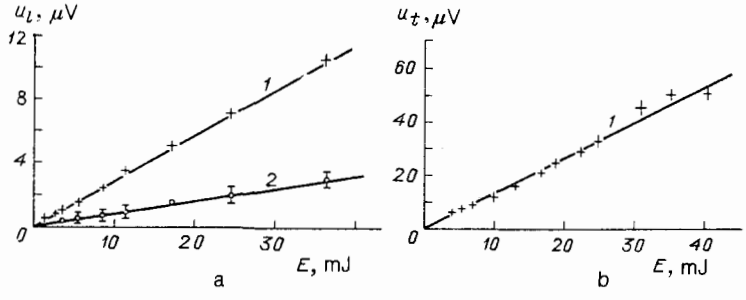

FIG. 3. The change in acoustic pulse amplitude depending on the energy in the laser beam. a—For a longitudinal wave pulse. b—For a transverse (shear) wave pulse. *1*—aluminum, *2*—steel.[46]

Numerous experiments were conducted in order to study the characteristics of acoustic signal from moving TRSS. Fig. 4 shows as an illustration the dependence of the amplitude of an acoustic signal excited by laser radiation in water in the Cherenkov direction in the Mach wave (in the case of supersonic movement of a laser beam over a liquid surface) on the energy of a laser pulse. It follows from the theory that this dependence has to be linear as the effective laser pulse is very short due to the beam motion and the acoustic signal takes on the universal form. The data given in Fig. 4 not only confirm the theoretical conclusions but also show that the experiments were conducted under conditions when the linear theory of laser thermo-optical excitation of sound by a supersonically moving beam still holds, i.e. the density of the released laser radiation energy is still not very great.

4.1.6. Sound excitation by x-rays (synchrotron radiation) in metals

The first results of the experimental studies of sound excitation by x-rays can be found apparently in Refs. 47–49. The most complete description of the results is contained in Ref. 49. There is nothing extraordinary in the application of x-rays to sound excitation in condensed media and especially in metallic samples after the research on laser sound excitation. Sound is excited by electromagnetic radiation in both cases. However, the depth of penetration of x-ray quanta in metallic samples depends on the sample physical parameters (atomic number of the substance) and on the energy of the radiation quanta in contrast to laser radiation. For example, the penetration depth in aluminum for x-rays with an energy of 10 keV is about $1.4 \cdot 10^{-2}$ cm and for laser radiation it is approximately $3.76 \cdot 10^{-7}$ cm. This difference can be significant from the point of view of practical applications.

The synchrotron of the Cornell University (USA) served as the x-ray source in the experiments of Refs. 47–49. Synchrotron radiation in the x-ray range was used. The radiation used in the experiment of Ref. 49 arose due to the motion of an electron "bunch" in the circular storage ring of the synchrotron.

The x-rays used in the experiments had the following parameters: the quanta energy was 10 keV, the pulse duration was $0.16 \cdot 10^{-9}$ s and the pulse repetition period was about $2.56 \cdot 10^{-6}$ s. This period was determined by the time of movement of the electron "bunch" in the synchrotron storage ring. The energy of a beam of photons (in a pulse) of x-rays incident directly upon a sample-target was $1.2 \cdot 10^{-6}$ J per pulse. Fig. 5 shows a block-diagram of the experiment. The x-rays (synchrotron radiation) passing through a collimator (*1*) was incident upon a protecting screen (*2*) and then on a sample-target (*3*). A wide-band piezotransducer (*4*) was installed at the opposite side of the target. The signal from the transducer output came to the input of a preamplifier (*5*) with the band-width from 0.01 to 2 MHz. Then the signal came to an integrating amplifier (*6*) and a data storage system (*7*). A synchronization signal from the x-ray detector (*8*) was used to increase the noise stability of the measurements. The detector response time was not more than 10^{-9} s. The synchronization signal came to the amplifier and integrator (*6*) which included an analog-code converter. The minimum x-ray beam dimensions on the target surface were 3 mm.

The sample targets had the form of a disk with a diameter of 5.72 cm and a thickness of 1.52 cm. Aluminum, stainless steel, copper, bronze and titanium were used as the target material. Aluminum cylindrical samples with a length of 10.2 mm were used for the measurements of the directivity pattern of the thermoradiation sound source in a solid. It is appropriate to note that the thickness of the disc targets was

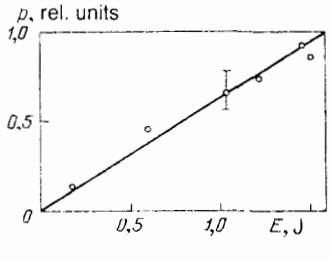

FIG. 4. The dependence of the sound pressure amplitude in the Cherenkov direction on the energy of the laser pulse.[38]

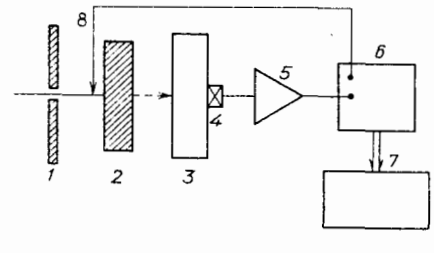

FIG. 5. Block diagram of the experimental setup (see the text for explanations).[49]

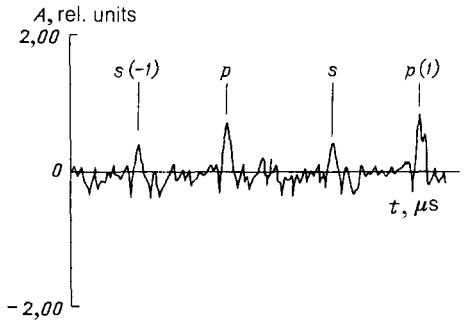

FIG. 6. Record of signals from a thermoradiation sound source in a stainless-steel target at the piezotransducer output after digital filtration in a wide band and differentiation. *p*—the pulses of longitudinal waves, *s*—the pulses of transverse waves.[47]

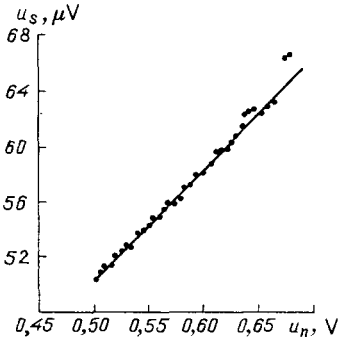

FIG. 7. The dependence of an acoustic signal amplitude (longitudinal waves) generated by a beam of x rays on the value of the photon energy in the beam. The amplitude of the electric voltage is given along the ordinate and the electric voltage (the beam energy) is given along the abscissa. The value of the electric voltage increases in direct proportion to the x-ray beam energy.[49]

considerably greater than the penetration depth of x rays into the target material ($\mu^{-1} = 1.4 \cdot 10^{-2}$ cm in aluminum, as mentioned above). Characteristic times of sound passage along the TRSS dimensions in the targets were greater than the x-ray pulse length, as we shall see below. In other words, the conditions for sound excitation in solids by very short pulses of penetrating radiation were satisfied.

A typical record of a signal form from the wide-band transducer after digital filtration is given in Fig. 6. Zero time corresponds to the arrival of the x-ray pulses at the sample-target surface. The letter *p* denotes the ultrasound radiation-acoustic pulse from longitudinal waves and *s* is for the pulse from transverse waves, $s(-1)$ corresponds to the transverse waves pulse caused by the action of a preceding x ray pulse incident upon the target and $p(1)$ is for the longitudinal waves pulse from the next x-ray pulse. We recall that the repetition period of x-ray pulses was 2.56 μs.

Fig. 7 shows the dependence of the ultrasound pulse amplitude on the energy in the x-ray beam incident on the steel target. The ordinate axis shows the voltage proportional to the ultrasound signal amplitude, and the abscissa axis shows the voltage characterizing the energy in the x-ray beam. The beam energy is directly proportional to the amplitude of the current in the particle beam of the synchrotron and the electric voltage value is directly proportional to the current in the synchrotron beam. The above data are obtained by averaging of results (at each point) of at least a hundred individual measurements.

Measurements of the dependence of the amplitude (peak) values of the ultrasonic signal on the aperture dimensions of the x-ray beam were conducted. The experimental setup was that the beam passed before the sample-target through a narrow slit of constant height of 3 mm, while the slit length varied from 3 to 30 mm. The results of measurements for a stainless steel target are shown in Fig. 8a, and for brass and aluminum—in Fig. 8b. One can see that in the beginning the linear dependence of the amplitude peak value of the ultrasonic thermoradiation signal on the slit length (aperture) is observed as it follows from the theory, and then this linear dependence is violated. The authors of Ref. 49 have established experimentally that in the case of a considerable increase of the slit length (x-ray beam aperture) the ultrasonic signal form changes significantly, while for initial alterations of the slit length this form remains practically constant. The violation of the linear dependence of the ultrasonic signal peak amplitude on the linear dimension of the x-ray beam aperture in the case of a significant increase of the aperture (slit) length is explained by the acoustic signal form alteration.

All the experimental data of Ref. 49 presented above agree completely with the conclusions of the theory mentioned above. Indeed, it follows from the theory that in the case of acoustic signal excitation in a solid elastic half-space by penetrating radiation pulses of very short duration the acoustic signal amplitude varies in direct proportion to the penetrating radiation pulse energy. Just these conditions were realized experimentally. The penetration depth of x rays into the target material was considerably less than the target dimensions and the pulse duration was very small compared with the temporal dimensions of the thermoradiation sound source created in the target by the action of the x-

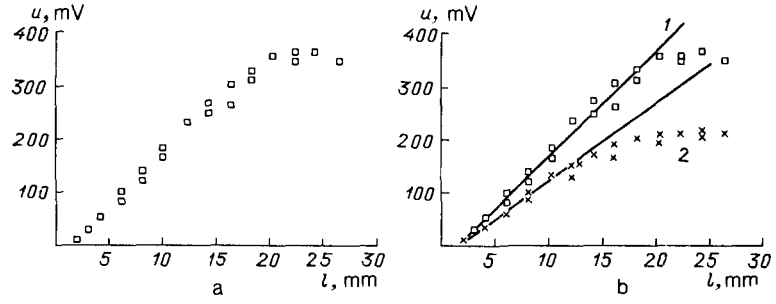

FIG. 8. The dependence of the maximum (peak) value of the acoustic signal amplitude from longitudinal waves in a sample-target on the aperture dimensions of the x-ray beam: a—Steel. b: *1*—brass, *2*—aluminum. The vertical axis is for the signal amplitude and the horizontal axis is for the slit (aperture) length.[49]

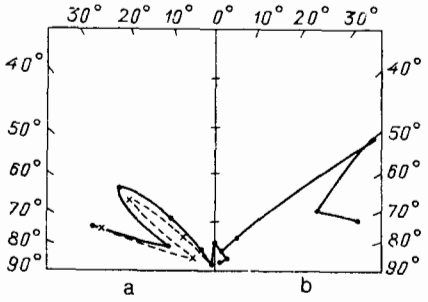

FIG. 9. Polar characteristics of a thermoradiation acoustic source in aluminum for different dimensions of the x-ray beam. a—The beam dimensions are 3×3 mm^2. b—The beam dimensions are 2×1.5mm^2. The measurements were conducted using longitudinal waves and the frequency of x-ray pulses was 1.2 MHz.[49]

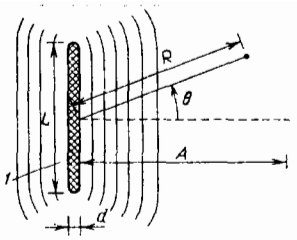

FIG. 10. Schematic diagram of sound generation by a proton beam.[52] *I* is the energy deposition region (thermoradiation array), *L* is the proton track length, *d* is the diameter the proton beam region, *R* is the distance to the observation point, *A* is the characteristic distance to the boundaries between the near and far wave zones.

ray pulses. It also follows from the theory that an increase in one of the beam aperture (slit) linear dimensions at constant radiation intensity in the beam incident upon the target must lead to a linear increase of the acoustic signal amplitude. Just such dependence was observed in the experiments of Ref. 49.

The authors of Ref. 49 have also made measurements of the TRSS directivity pattern (angular dependence of an acoustic signal amplitude) in a solid. The results are given in Fig. 9a and b. In the first case (Fig. 9a) the beam dimensions were 3×3 mm and in the second case (Fig. 9b) they were 3×1.5 mm. These characteristics correspond to longitudinal waves in a sample-target. As it was noted justly in Ref. 49, the polar characteristics are very similar to the angular acoustic characteristics of the opto-acoustic source arising in a solid under the action of short pulses of focused laser radiation.

4.1.7. Sound oscillations generated in a condensed medium by proton beams

Sound excitation in a condensed medium by a proton beam was repeatedly studied experimentally. Here we shall consider in detail the results given in Refs. 50–52.

The author of Ref. 52 conducted extensive experiments on sound excitation in liquids by proton beams at the accelerators of Brookhaven National Laboratory (USA) and Harvard University (USA). A proton beam extracted from an accelerator was directed through a collimator to a tank with a liquid. The acoustic signal was received by a hydrophone provided with a preamplifier and an amplifier-recorder. The measurements were conducted in a pulsed mode.

The experiments on sound excitation in water by a proton beam with an energy of 200 MeV were conducted with the help of the linear accelerator of the Brookhaven National Laboratory. The tank dimensions were considerably greater than the proton range and the spatial dimensions of the acoustic signal in water, and this allowed one to realize the spatial-temporal selection of a direct acoustic signal and signals reflected from the tank walls. The proton range in water was about 30 cm. The beam operation time (pulse duration) varied from 3 to 200 μs and the energy release was from 10^{10} to 10^{21} eV. The proton beam diameter was fixed and equal to 4.5 cm.

Analogous experiments were conducted at the cyclotron of Harvard University using a proton beam with an energy of 158 MeV. In this case the energy release was 10^{15} eV while pulse duration was 50 μs and the proton range in water was ~16 cm. Cyclotron experiments were conducted not only with water, but also with various liquids under different conditions (at different values of liquid temperature and static pressure). The tank dimensions in these experiments were less than the dimensions of the tank used in the experiments with the linear accelerator, but they were still considerably greater than the sound wavelength.

The third series of experiments was performed with the accelerator of Brookhaven National Laboratory using proton beams with an energy of 28 GeV (a beam with a very short pulse duration). The value of energy release was less than 10^{19} eV as in the experiments with the linear accelerator. In the typical experiment of this series $3\cdot10^{11}$ protons passed the distance of 20 cm in water during one pulse; the beam diameter was varied from 5 to 20 cm and the time of energy release (pulse duration) was less than 2 μs. In contrast to the cyclotron measurements the proton pulse duration was always less than the sound propagation time along the beam diameter, i.e. the conditions of sound excitation by a very short pulse of penetrating radiation were realized.

The experimental setup is shown in Fig. 10. The measurements have shown that in the near wave zone of a thermoacoustic antenna the acoustic signal has the form of an N-wave as should have been expected.

The dependence of the acoustic signal (N-wave) duration on the beam diameter value was measured in the experi-

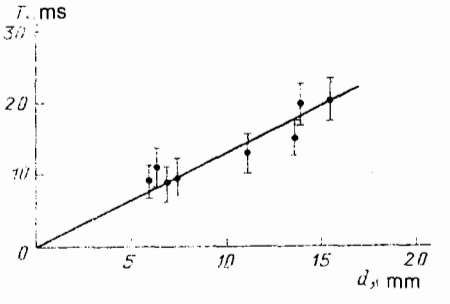

FIG. 11. The dependence of the acoustic signal duration on the diameter of the proton beam.[52]

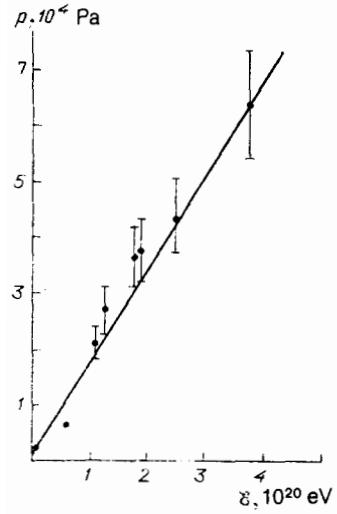

FIG. 12. The dependence of the acoustic signal amplitude in water on the value of the deposited energy.[52] $T = 20$ °C, $d = 4.5$ cm, $R = 100$ cm, $\tau = 10\,\mu$s.

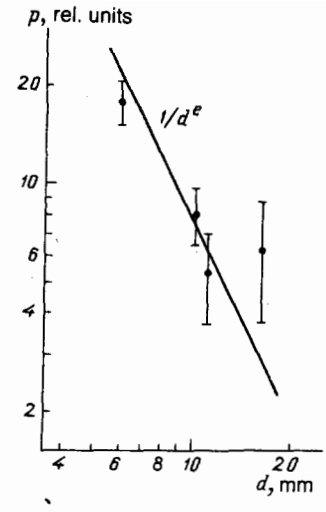

FIG. 14. The dependence of the acoustic signal amplitude on the beam diameter.[52]

ments with the proton beam of an energy of 28 GeV. The observed dependence is shown in Fig. 11. It can be seen that this dependence is linear. This corresponds to the theory conclusions: under the condition $\tau < \tau_a$ the acoustic signal duration is directly proportional to the beam diameter (radius).

Fig. 12 shows the experimental data characterizing the dependence of an acoustic signal amplitude in water on the value of the energy release in the case of a proton beam of very short duration ($\tau \approx 10\,\mu$s). It follows from the theory that a linear dependence of the signal amplitude on the penetrating radiation energy should be observed, and this fact has been confirmed experimentally. The analogous data are given in Fig. 13, but for a proton beam with lower energy release. The experiments were conducted at the Harvard University cyclotron.

It follows from the theory that at constant beam energy (power) the acoustic signal amplitude must vary inversely in proportion to the square of the beam diameter. Fig. 14 shows the experimental data confirming this dependence.

It follows from the equation of sound generation in condensed media by penetrating radiation that the sound signal amplitude increases in direct proportion to the value of the ratio of the thermal volume expansion coefficient to the specific heat of a medium. An experimental confirmation of such dependence is obtained in Ref. 52 (see Fig. 15).

Another confirmation of the thermoradiation mechanism of sound generation by penetrating radiation under moderate densities of the energy evolved in a medium is the dependence of TRSS acoustic signal amplitude on temperature obtained in the experiments of Ref. 52. Figs. 16 and 17 show this dependence for a proton beam in water. The special feature of the observed dependence is that the value of thermal expansion for water must become zero at 4 °C. Meanwhile, the amplitude of the acoustic signal generated by a proton beam becomes zero at approximately 6 °C. This fact can be explained by the existence of an additional sound generation mechanism and this is the microstrictional compression of a medium under the action of ionizing particles on a medium,[53,54] that leads to the effect of compensation of

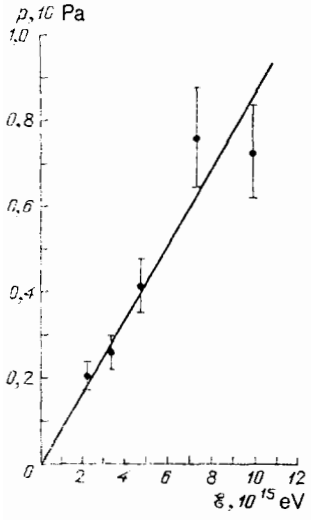

FIG. 13. The dependence of the acoustic signal amplitude on the energy deposition.[52] $T = 20$ °C, $d = 1$ cm, $R = 8$ cm.

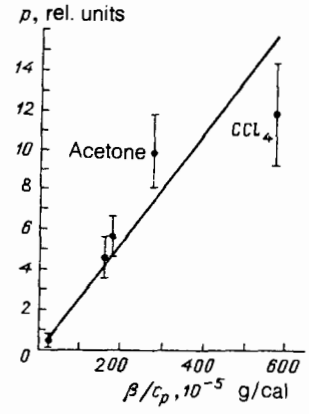

FIG. 15. The dependence of the acoustic signal amplitude on the value of the ratio β / C_p.[52]

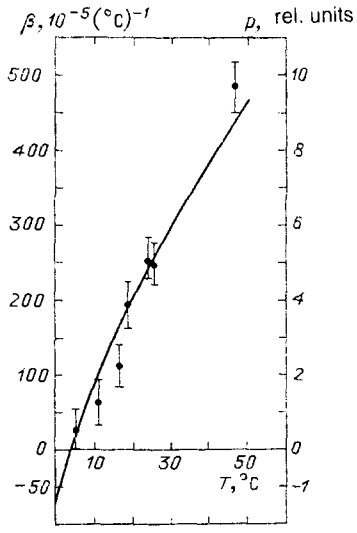

FIG. 16. The dependence of the thermal expansion coefficient β (solid line) of the acoustic signal amplitude p (circles) on the temperature.[52]

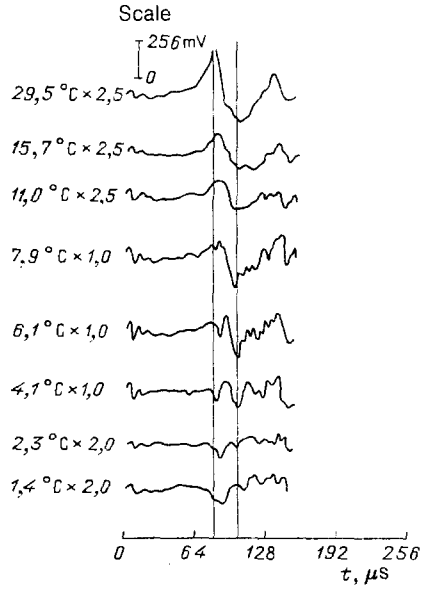

FIG. 18. The form of the acoustic signal at different temperatures in the frequency band from 7 to 80 kHz.[51]

the thermal expansion of the medium caused by the thermoradiation mechanism at the temperature of 6 °C.[51]

The authors of Ref. 51 have conducted careful experiments in order to establish the presence of a nonthermoradiation sound generation mechanism in water under the action of a proton beam. The experiments were conducted at the Brookhaven National Laboratory accelerator using a beam of high-energy protons of 20 GeV. The discharge time in a beam (proton pulse duration) was varied from 1.5 to 3 μs that was considerably less than the time of sound passage along the beam diameter (8×10 mm^2 and 5×7 μs respectively). The proton beam was introduced into a special Dewar vessel with water, the temperature of which could be altered and these alterations were carefully controlled. Sound pulses were received by a miniature high-sensitivity hydrophone made of zirconate-titanate piezoceramic with the pass band from 0.1 Hz to 120 kHz and provided with an amplifying and recording device.

The idea of the experiments was to clear up how the sound pulse form changes with changing water temperature in the temperature interval close to the critical temperature when the volume expansion coefficient of water becomes zero and then changes its sign to the opposite one. Preliminary statements based on the ideas of possible nonthermoradiation (nonthermoelastic) mechanisms were made that the power spectra of the signals of thermoradiation and nonthermoradiation "origin" must under certain conditions differ (in their basic energy-carrying part) as the form and duration of pulses of different origin differ.

These ideas have been realized in experiments. It was established that in the case of sound excitation in water by a proton beam with the characteristics given above and registration of the generated acoustic signal in a wide band, the signal amplitude becomes zero at 6 °C (see Fig. 18). However, in the case of registration in a relatively narrow band corresponding to the energy-carrying band of the N-wave caused by the thermoradiation mechanism (this band is determined by the time τ_a of passage of sound along the transverse dimensions of the beam) the acoustic signal becomes zero at the temperature of 4 °C (see Fig. 19) that corre-

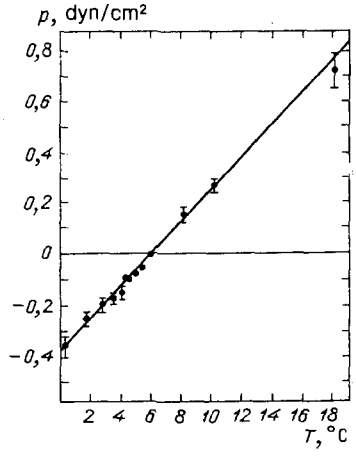

FIG. 17. The dependence of the acoustic signal amplitude on the temperature.[52]

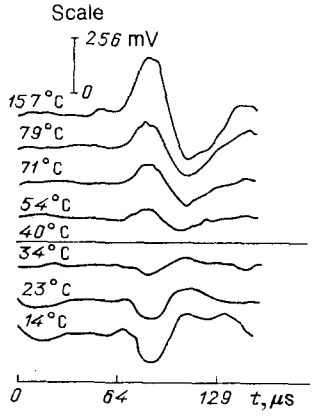

FIG. 19. The form of the acoustic signal at different temperatures in the frequency band from 7 to 40 kHz.[51]

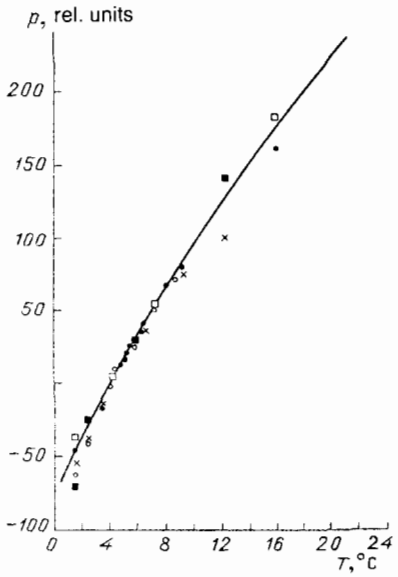

FIG. 20. The dependence of the acoustic signal amplitude on the temperature in the frequency band from 7 to 40 kHz.[51]

sponds to the temperature dependence of the thermal expansion coefficient of water (Fig. 20).

Very interesting studies of sound excitation in water by a proton beam have been conducted by the authors of Ref. 50. The measurements were performed with the help of the beam of the ITEP (Institute of Theoretical and Experimental Physics, USSR) synchrotron. Protons of the energy of 200 and 190 MeV were used. The collimator diameter was 4 cm. Water temperature was controlled. The beam operation time was 100 ns that was far lower than the acoustic pulse duration (~ 100 μs). The total energy release was varied from $8 \cdot 10^{15}$ to $23 \cdot 10^{19}$ eV. The acoustic signal was measured by a hydrophone and a registration device with the frequency band from 0.1 to 80 kHz in the near wave zone of the TRSS created by the proton beam in water.

The amplitude of the N-signal positive half-wave was recorded. Fig. 21 shows the acoustic signal dependence on the proton energy obtained in the experiments. The data of other authors who conducted analogous measurements using proton, laser and electron beams of different energy[55-57] are given on the same figure for comparison.

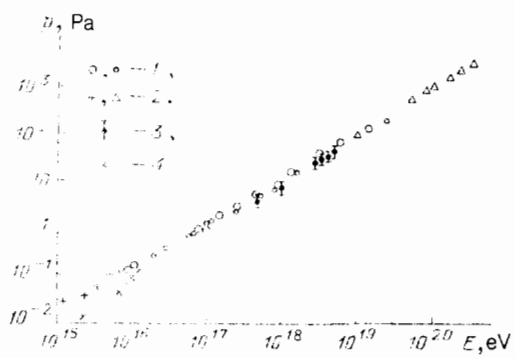

FIG. 21. The dependence of the acoustic signal amplitude on energy. The data of the authors of *1*—Ref. 50, *2*—Ref. 55, *3*—Ref. 56, *4*—Ref. 57.

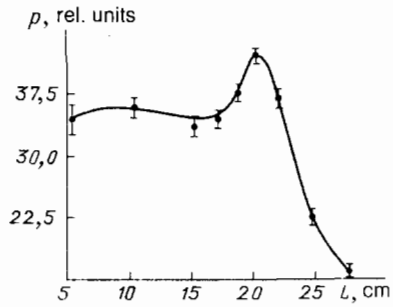

FIG. 22. The dependence of the acoustic signal amplitude on the hydrophone position along the beam axis. The distance to the beam axis is 7 cm.[50]

Fig. 22 shows the dependence of the acoustic signal amplitude in the TRSS near wave zone on the hydrophone position along the beam axis obtained by the authors of Ref. 50. The proton absorption mechanism corresponding to the so-called Bragg peak at the end of the proton range is seen clearly. The presence of such a mechanism is caused by the known dependence of ionization losses on the proton energy. The dependence of losses of polonium α-particles in air on the residual range is given in Fig. 23 for comparison (see p. 207 in Ref. 34). A good correlation of the data given in Fig. 22 and Fig. 23 can be seen.

The experimental data given above characterizing sound generation by protons in a condensed medium concerned mainly the case when the dimensions of the volume of the medium are large compared with the proton range in the medium. Meanwhile, the situations when the ratio of the range to the target thickness changes within the range of variation of the proton energy, are of interest. Such experiments were conducted by the authors of Refs. 58, 59. As should have been expected from physical considerations and, as is the consequence from the theory, a maximum must be observed on the curve characterizing the dependence of the acoustic signal amplitude on the value of the energy of protons incident on a target plate. The authors of Ref. 59 observed this maximum and have called it the acoustic peak of protons. The physical nature of this peak is essentially the same as of the Bragg peak on the curve characterizing proton absorption in a substance. The experiments of Ref. 59 were conducted at the ITEP synchrotron. Relatively low-fre-

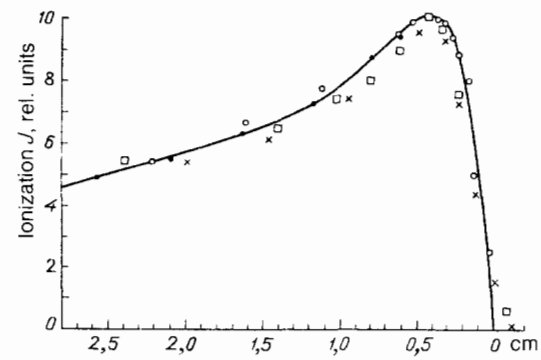

FIG. 23. The dependence of ionization created by polonium α-particles in air on the residual track length.[34]

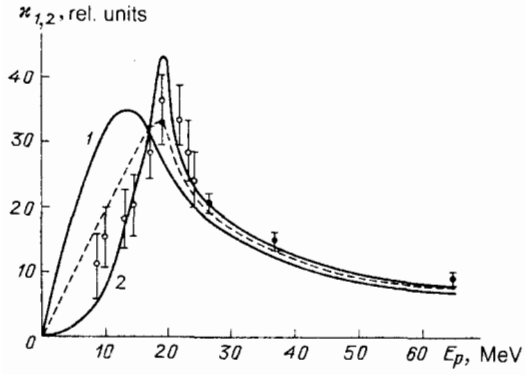

FIG. 24. The dependence of the acoustic signal amplitude (displacements of the plate sides) (relative units) on the proton energy for the aluminum plate ($h = 0.2$ cm).[59]

quency acoustic oscillations ($f = 66$ kHz) arising in an aluminum target plate (the plate thickness was 0.2 cm) were registered. The proton pulses (the pulse duration was $\tau = 20$ μs) with an initial energy $E_p = 24.6$ MeV in a beam of diameter $d = 0.75$ cm were incident after a collimator on the plate center. The proton beam energy was varied by passing the beam before the collimator through a cassette containing retarding plates made of copper foil.

Fig. 24 shows the dependence of the displacements of the front and rear sides of the plate (curve *1* and curve *2* respectively). The curves *1* and *2* were obtained by a calculation based on the simplest one-dimensional model of the thermoelastic (thermoradiation) sound excitation by protons in a plate. The circles show experimental data. Empty circles correspond to the experiments of Ref. 59. The maximum on the curve *2* corresponds to proton energy for which the proton range in aluminum is equal to the plate thickness ($E_p = 19$ MeV). The dotted curve corresponds to half the sum of the displacements x_1 and x_2 which is proportional to the absorbed energy of protons according to the estimates of Ref. 59. The black circles show experimental data published a little earlier in Ref. 58. These data can serve as an illustration demonstrating an increase in ionization losses due to the interaction of the proton beam with a substance, and an increase of excited sound amplitude. The results of these experiments are given in Fig. 25 which shows the dependence of the acoustic signal amplitude generated in an aluminum plate by protons with the initial energy $E_p = 70$ MeV on the thickness of a plexiglas plate absorbing the radiation. The absorbing plates were installed in the proton beam path before the aluminum plate. The experiments were conducted at the accelerator of Physical-Technical Institute of the Ukrainian Academy of Sciences. The maximum value of the acoustic signal amplitude corresponds to the Bragg peak. The results of calculations concerning these experimental data given above in Fig. 24 and performed a little later,[59] showed that the maximum value corresponds to such an energy of protons incident on the aluminum target cell at which the proton range in the aluminum plate is equal to its thickness. The results of Refs. 58, 59 correlate with the conclusions of the theory that the condition of the equality of the radiation length and the plate thickness is optimal in the case of sound generation by penetrating radiation.

4.1.8. Sound generation in metals by electrons, positrons and γ-quanta

Sound excitation by electrons was studied by the authors of the first papers on radiation acoustics. The theory describing the Cherenkov acoustic radiation by an electron moving uniformly with a supersonic velocity in a metal was considered first.[4,5] The first radiation-acoustic experiments also concerned sound excitation by an electron beam in a solid. It is characteristic that these investigations were conducted practically simultaneously with experiments (the first ones also) on laser excitation of acoustic waves in solids.[9]

Numerous experimental studies of sound excitation in condensed media by electrons including excitation by electron beams in metals, were conducted after that. These experiments were performed with different accelerators over a wide range of energy under conditions when sample target thickness was greater than the radiation length (thick target plates), or with thin plates (see, for example, Refs. 15, 60, 61. Acoustic wave excitation in liquids by electron beams was studied by the authors of Ref. 14. Papers were published in recent years in which the nature of acoustic waves generated by an electron beam in crystals and natural solids is discussed.[62-65]

We shall give below some typical results of the studies of acoustic wave excitation by electrons, positrons and γ-quanta in metals.[61] The experiments were conducted using linear accelerators of the Physical-Technical Institute of the USSR Academy of Sciences. The beam of electrons (positrons) from a linear accelerator was incident upon a plate of a metal under investigation. A piezoreceiver was installed on the plate. The receiver was connected to signal amplifying and recording equipment. The typical duration of a bunch of particles incident on a sample target was $\tau = 1$ μs. A flow of bremsstrahlung was produced in a tantalum target $5.3 \cdot 10^{-12}$ cm thick by an electron beam with an energy

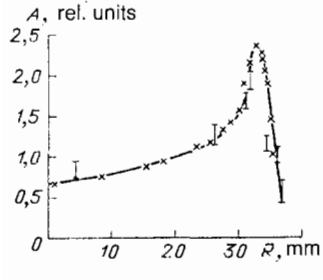

FIG. 25. The dependence of the signal on the thickness R of a plexiglas absorber. The initial proton energy is $E_p = 70$ MeV.[58]

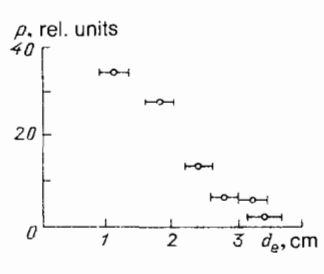

FIG. 26. The dependence of the acoustic signal amplitude on the diameter of the electron beam on the target.[61]

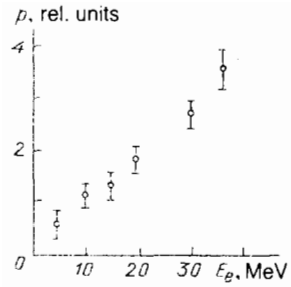

FIG. 27. The dependence of the acoustic signal amplitude on the electron energy for a thick aluminum plate.[61]

$E_\gamma = 620$ MeV. The bremsstrahlung beam after passing through several collimators had an average transverse dimension (diameter) $d = 1.5$ cm on the surface of the investigated target plate.

Fig. 26 shows the dependence of the acoustic signal amplitude on the electron beam diameter on the target that is a lead plate 0.2 cm thick. The plate was thin, i.e. its thickness was less than the range of electrons in lead. The experiments were conducted at an electron energy of $E_e = 20$ MeV, with a fixed number of particles in the beam and with the radiation pulse duration $\tau = 2\,\mu$s. Thus, the total energy (power) of the electron beam stayed constant although the beam diameter on the plate surface was varied, and the intensity varied in inverse proportion to the square of the beam diameter as it should in the TRSS near wave field.

These experimental data agree with the results of the thermoradiation sound excitation theory as in the cases of sound excitation by proton and synchrotron radiation (x ray) beams considered earlier.

Measurements data of the acoustic signal amplitude dependence in a thick aluminum plate ($h = 5$ cm) are given in Fig. 27. The plate thickness was of the order of the electron range in aluminum and the radiation pulse duration was less than the time of sound passage along the beam dimensions in the plate. The observed acoustic signal amplitude varies linearly with the increase of the electron energy in the beam, just as predicted by the theory.

The dependence of the acoustic signal amplitude in a thick lead plate on the number of electrons (positrons) in the penetrating radiation pulse is shown in Fig. 28. The plate thickness was $h = 5.0$ cm. The particle energy was $E_e = 620$ MeV. Since the total energy in a radiation pulse is directly proportional to the number of particles the experimental results correspond to the theory as in the previous case.

Fig. 29 shows the dependence of the acoustic signal amplitude on the electron energy for a thin aluminum plate

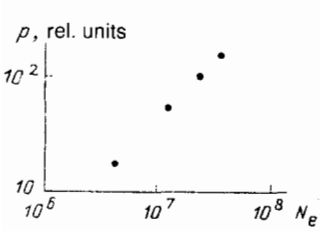

FIG. 28. The dependence of the acoustic signal amplitude on the number of electrons for a thick ($h = 5.0$ cm) lead plate ($E_e = 620$ MeV).[61]

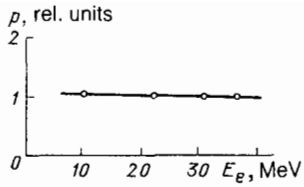

FIG. 29. The dependence of the acoustic signal amplitude on the electron energy for a thin aluminium plate ($h = 0.2$ cm).[61]

($h = 0.2$ cm). In this case the plate thickness is small compared with the radiation length. The electron energy in this experiment was lower than critical, i.e. $E_e \ll 40$ MeV. Therefore, the basic losses in the process of electron beam absorption in aluminum are ionization losses. In this case the total number of secondary or δ-electrons in the energy range from 10 to 30 MeV does not change. The absence of an acoustic signal amplitude dependence on the the energy of the electrons in the beam is explained just by this fact.

Finally, Fig. 30 shows the dependence of the intensity (and not the amplitude, as above!) of acoustic oscillations excited in a thick lead plate on the total number N_γ of equivalent photons of γ-radiation at $E_\gamma = 620$ MeV. One can see that also in this case a linear dependence of the acoustic signal amplitude on the energy of γ-radiation photons is observed.

The data on sound excitation in a solid by a beam of low-energy electrons are given in Ref. 66. These data deserve our attention also because the target was an aluminum cylinder with a mass of 1000 kg. This cylinder had the first quadrupolar oscillation mode of 10 rad/s and a quality factor of 10^5. The cylinder oscillations were recorded by a capacitive transducer. The signal was stored. An electron gun was the source of electrons. The gun was positioned close to the lateral surface of the cylinder and accelerated electrons up to the energy of $E_e = 0.5$ keV. The current pulse duration was $\tau = 8\,\mu$s. The interest in the study of the action of low-energy particle flows on such massive bodies arose due to the problem of gravitational wave detection with the help of detectors that are massive elastic bodies. The dependence of the amplitude of acoustic oscillations in the cylinder on the electron beam energy is shown in Fig. 31. We can draw a conclusion based on the above data (as the authors of Ref. 66 do themselves) that the acoustic signal dependence on the electron energy is linear.

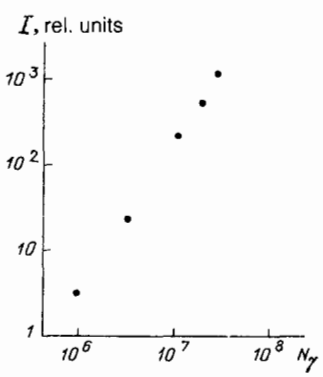

FIG. 30. The dependence of the acoustic signal intensity on the total number of equivalent photons at $E_\gamma = 620$ MeV for a lead plate of thickness $h = 5.0$ cm.[61]

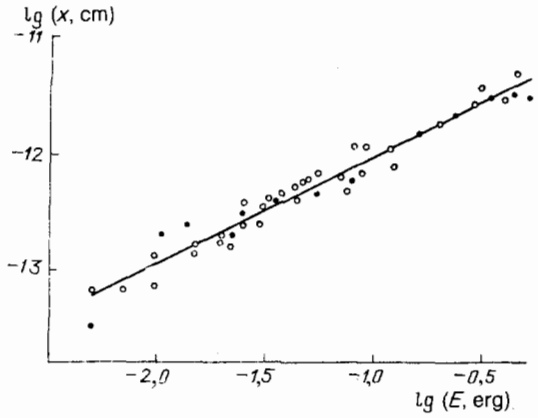

FIG. 31. The dependence of the amplitude of acoustic oscillations (x) in a cylinder on the energy of the electron beam.[66]

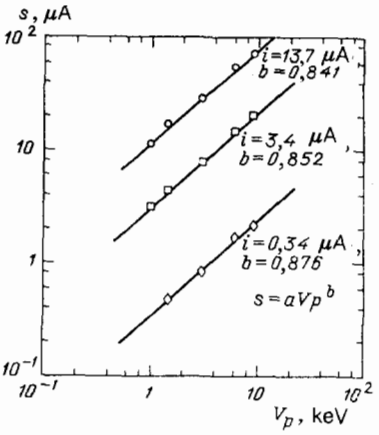

FIG. 33. The dependence of the acoustic signal amplitude s in aluminum on the energy of the beam of Ar^+ ions at different values of the current in the beam.[68]

Thus, the above data testify in favor of the thermoradiation mechanism of sound generation by electron (positron) and γ-quanta beams and agree with the theoretical concepts.

4.1.9. Excitation of sound in metals by ion beams

The papers of Refs. 67–68 were published relatively recently. The authors studied sound excitation by ion beams in metals. The results of the experimental studies of acoustic waves generation by a beam of Ar^+-ions in aluminum given in Ref. 68 are the most characteristic. An aluminum disc with a diameter of 1.4 cm and thickness of 0.3 cm was used in the experiments. A piezoreceiver made of PZT ceramics was fixed on one of the disc sides. A beam of Ar^+-ions was incident on the opposite side. The ion energy was varied from 1 to 10 keV. The value of the current in the beam-target-piezoreceiver circuit could be varied from 0.3 to 14 μA at a fixed ion energy (in other words, the number of particles in the beam was varied). The modulation frequency of the ion beam intensity could also be varied from 15 Hz to 20 kHz. The diameter of the Ar^+-ion beam on the target (aluminum disc) surface was 300 μm. Some experimental results are given below.

Fig. 32 shows the dependence of the acoustic signal amplitude at the piezoreceiver output on the current value in the beam at a modulation frequency of its intensity of 2 kHz. The parameter is the value of the energy of the ions in the beam. The dependence of the acoustic signal amplitude s on the current value i_p can be approximated by the expression $s = ai_p^b$ where b is the index characterizing the straight line slope and is equal to $b = 0.96$ approximately, and a is a coefficient. Analogous dependences were observed in the entire range of variation of the beam intensity modulation frequency from 15 Hz to 20 kHz.

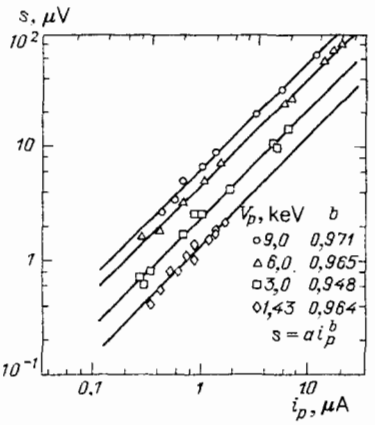

FIG. 32. The dependence of the acoustic signal amplitude s in aluminum on the current value i_p in the beam of Ar^+ ions at different energy of particles in the beam. The modulation frequency of the beam intensity is 2 kHz.[68]

Fig. 33 shows the data characterizing the dependence of the acoustic signal amplitude at the piezoreceiver output on the value of the voltage V_i which characterizes the ion energy. The parameter was the current value in the beam (the number of particles). The observed dependences can be described by the relationship $s = aV_p^b$ as was done above, where the value of the index is also approximately equal to $b = 0.96$.

These experiments show that a practically linear dependence of the acoustic signal amplitude on the ion energy (or the number of particles) is observed. The authors associate the certain small difference (the index is after all not equal to unity) from a linear dependence with the fact that a so-called dynamic mechanism, i.e. the mechanism of a direct transfer of the beam particle momentum to a metallic target, takes part in acoustic wave excitation in metals by heavy ions besides the thermoradiation or thermoelastic mechanism. A "negative" influence of the striction mechanism is possible also. Their role becomes less and less significant as the particle energy increases and, therefore, the dominant mechanism at moderate densities of the energy of the penetrating radiation being absorbed in a substance and at high particle (ion) energy is the thermoradiation mechanism (see Note 4).

4.2. Microshock waves generated in a condensed medium by penetrating radiation

In some cases the passage of penetrating radiation through a substance can be accompanied by microshock waves. So, the passage of fission fragments through a liquid can be accompanied by shock wave formation along the entire track of the fission fragments.[69] On the other hand, delta electrons appearing in the process of passage of ionizing par-

ticles through a liquid form overheated microregions (thermal peaks) in it. The explosive expansion of these peaks gives birth to a shock wave.[70] Shock wave formation is an essentially nonlinear phenomenon. The theory of such processes is as yet far from complete. Let us cite some parameters of shock waves from delta electrons according to Ref. 70.

It is necessary for the formation of a microregion capable of explosive expansion that the energy lost by an ionizing particle be localized initially in a sufficiently small volume. This condition can be satisfied for delta electrons knocked off by an ionizing particle. The delta electron track length l_δ (in centimeters) depends on its energy E_δ (in electronvolts) in the following way:

$$l_\delta = 0{,}58 \cdot 10^{-12} A E_\delta^2 / \rho Z, \tag{30}$$

where ρ is the density of the medium (water), Z/A is the ratio of the number of electrons to the molecular mass. The form of the trajectory of a delta electron as its energy decreases differs more and more from a rectilinear one and becomes more like a ball of thread. For example, the average track length of an electron is 0.5 l_δ already at $E_\delta = 10$ keV. The number ν of water molecules along the length l_δ is determined as follows:

$$\nu = \frac{l_\delta}{d} = \frac{l_\delta}{2}\left(\frac{4\pi\rho N_A}{3A}\right)^{1/2}; \tag{31}$$

here d is the diameter of the spherical volume V_1 occupied by a single water molecule, N_A is the Avogadro number. The delta electron track is situated within a sphere if the electron energy is sufficiently low. The volume of this sphere V_0 is determined by the formula $V_0 = \nu V_1 = l_\delta A/(\rho N_A d)$. The energy ΔE transferred on the average to a single molecule is equal to $\Delta E = E_\delta d / l_\delta$. If we choose (proceeding from reasonable assumptions) for water the value of $\Delta E = 30$ eV at which microexplosive formation of bubble-nuclei takes place, then the parameters for which an explosive expansion of an overheated microregion in water is possible will have the following values: $E_\delta = 1.23$ keV, $\nu = 41$, $V_0 = 1.23 \cdot 10^{-21}$ cm^{-3}. The radius of a sphere of such volume V_0 is equal to $a_0 = 6.64 \cdot 10^{-8}$ cm. The energy-release density q in the thermal peak determined by the formula

$$q = \frac{E_\delta}{V_0} = \frac{E_\delta A d}{l_\delta \rho N_A},$$

is $\sim 16.09 \cdot 10^{10}$ J/m^3 in this case. We would like to remind for a comparison that the calorific power of ordinary explosives is about $\sim 4.19 \cdot 10^9$ J/m^3.

According to the theory of underwater explosions the pressure in the shock wave can be written in the form

$$p_y(r, t) = p_{y,\max}(r)\exp(-t/\theta), \tag{32}$$

where $p_{y\,\max}(r)$ is the maximum pressure (in Pa), r is the distance from the center of the thermal peak spherical volume (in cm), t is the time, θ is the time constant (in seconds). One can show in this case that $p_{y\,\max}(r) = 7.37 \cdot 10^2 r^{-1}$ Pa, $\theta(r) = 1.07 \cdot 10^{-10}(7.18 + \lg r)$ at $r \gg 10^2 a_0$.

The pulse spectrum $p_y(r,t)$ has the following form:

$$|S_2(\omega)| = p_{y,\max}(r)[(\theta(r))^{-2} + \omega^2]^{-1/2}. \tag{33}$$

The spectrum is homogeneous at $\omega \ll 1/\theta(r)$ and can be written in the form

$$|S_2(\omega)| = p_{y,\max}(r)\theta(r).$$

The root-mean-square pressure $\langle p \rangle$ at a distance r from a unit thermal peak in water is $\langle p \rangle = 7.76 \cdot 10^{-8}(7.18 + \lg r)(1/r)$ Pa·Hz$^{-1/2}$ in the frequency band of 1 Hz. The number of these thermal peaks per unit track length of a relativistic electron is equal to the number of delta electrons of energy $E_\delta = 1.23$ keV. This number is equal to 17.32 cm^{-1} according to Ref. 45.

For example, one can obtain the following estimate for the acoustic signal intensity I_0 (in W/cm^2) in water from a single high energy particle forming on its entrance into the atmosphere an extensive atmospheric shower (EAS) consisting mainly of electrons:[70]

$$I_0 = 10^{-29} E_0 / R,$$

where E_0 is the particle energy (in eV), R is the distance from the EAS axis (in centimeters). At present recording of EAS by hydroacoustic radiation is apparently possible for $E_0 \geqslant 10^{17}$ eV.

4.3. "Bubble" sound generation mechanism

The possibility of sound generation in a liquid by ionizing radiation due to microbubble formation, oscillation and collapse on the tracks of ionizing radiation particles is discussed in a number of papers (Refs. 8, 71–75). The theory of the bubble sound generation mechanism is not completed yet. This is connected with the fact that a satisfactory description of the arising phenomena demands taking into account the complex processes of the dynamics of a single bubble and of a system of bubbles as well as nonlinear effects. Estimates show[73] that for microbubbles of the dimensions of the order of 10^{-7}–10^{-8} cm and for the interaction region with the characteristic dimension of the order of 1 cm, the main contribution to sound radiation is due to quasistable and not to collapsing microbubbles. In this case the acoustic signal will be similar to the thermal mechanism signal (but much stronger).

Recent experimental studies are indicative of the fact that the bubble mechanism of sound generation can apparently be realized under normal experimental conditions, i.e. at atmospheric pressure, room temperature and in stable liquids; the penetrating radiation consists of heavy particles, for example, of nuclear fission fragments.[75]

4.4. Dynamic sound generation mechanism

A momentum transfer from the penetrating radiation quanta to atoms of a medium takes place under the action of penetrating radiation on a substance. This transfer is accompanied by sound wave generation. This is the dynamic mechanism of sound generation.[76] The dynamic effect in crystals depends on the relative directions of the crystal axes and the velocity of the particle of the penetrating radiation.[77] The dynamic mechanism as well as the thermoradiation mechanism of sound generation, takes place with any kind of penetrating radiation and manifests itself both in liquids and in solids. However, the dynamic mechanism can play a fundamental role in solids due to the existence in them of transverse sound waves.

Just in the same way as in the case of the thermoradiation mechanism, the calculation of sound generation in solids (liquids) due to the dynamic mechanism, can be conducted within the framework of the linear approximation (see equations (2) and (3)) where F is the dynamic force applied to the unit volume. As can be seen from equations (2) and (3), the sources of both longitudinal and transverse waves arise in solids due to the dynamic mechanism in contrast to the thermoradiation mechanism when only sources of longitudinal waves exist. If radiation quanta consist of ultrarelativistic particles (e.g. photons) then the dynamic force is equal to $F = Q/u$ where u is the light velocity. One can see from equation (2) that for $F = Q/u$ for the majority of substances the ratio of displacements in sound waves caused by the dynamic mechanism (by the second term) to analogous displacements caused by the thermoradiation mechanism (by the first term) is of the order of the ratio of the longitudinal sound waves velocity to the light velocity c_l/u. Thus, in liquids the dynamic mechanism of sound generation contributes only a small correction to the sound field generated due to the thermoradiation mechanism. As for solids, in the cases when transverse waves cannot arise on account of reflection or scattering of longitudinal waves, it can be of fundamental importance to take into account the dynamic mechanism of sound generation equally with the thermal one.

4.5. Cherenkov mechanism of sound generation

When a particle moves in a medium with a velocity exceeding the phase velocity of wave propagation, it emits these waves (the Cherenkov radiation). The nature of the waves and of the particle determine the radiation intensity and its characteristics (dispersion and polarization). The Cherenkov sound radiation can be described phenomenologically if we introduce into the elasticity theory equation, a force per unit volume with which the particle acts on the lattice:[4]

$$\left(\Delta - \frac{1}{c_l^2}\frac{\partial^2}{\partial t^2}\right)\operatorname{div}\mathbf{u} = \frac{D}{\rho c_l^2}\Delta\delta(r - Vt), \tag{34}$$

where D is a constant with the dimension of energy and coinciding in order of magnitude with the energy binding the particle to the lattice; V is the particle velocity. There must be no transverse sound waves in the approximation under consideration as the transverse component of the force is identically equal to zero. The delta-like character of the force shows that due to screening the particle acts on atoms located within one cell. The particle emits longitudinal sound waves and the spectral density of the radiation energy $I(\omega)$ is proportional to the third power of the sound frequency:[4]

$$J(\omega) = \frac{D^2\omega^3}{4\pi\rho V c_l^4}.$$

A charged particle moving through a metal creates an electromagnetic field around itself which destroys the equilibrium of the conduction electrons. These electrons due to their binding with the lattice set the ions in motion.

If the particle velocity is greater than the sound velocity the Cherenkov mechanism leads to generation not only of longitudinal waves but also of transverse waves.[78] The spectral radiation densities $J_l(\omega)$ of longitudinal and $J_t(\omega)$ of transverse sound waves depend significantly on the particle and on the substance (metal) (on the particle velocity, on the mean free path of electrons in a metal, on the Debye frequency, on the Fermi energy, etc.). At low frequencies $J_t(\omega) > J_l(\omega)$. At some frequency $\omega = \tilde{\omega}$ the values of $J_t(\omega)$ and $J_l(\omega)$ become equal and at $\omega > \tilde{\omega}$

$$J_l(\omega) \gg J_t(\omega).$$

The frequency $\tilde{\omega}$ depends on the particle velocity V and on the electron mean free path l_e. The greater are l_e and V the greater is the value of $\tilde{\omega}$. The frequency $\tilde{\omega}$ attains its maximum value for ultrarelativistic particles $V \sim u$ at $l_e > \delta_0 (V_F/c_l)^{1/2}$, where V_F is the Fermi velocity of the metal conduction electrons ($\sim 10^8$ cm/s), $\delta_0 = 10^{-5}$ cm, $\tilde{\omega} \approx 10^{-4}\ \mathrm{s}^{-1}$.

The total intensity of radiation at all frequencies of transverse sound waves will be much less than the analogous value for longitudinal waves: $J_t(\omega) = J_l(\omega)(Vc_l/u^2) \ll J_l(\omega)$ and, therefore, the total intensity of sound radiation (at all frequencies) is determined by radiation of longitudinal sound waves.

The indirect character of sound wave excitation (particle—electromagnetic field—sound) does not change the Cherenkov character of their propagation along the corresponding cones $\cos\theta_{l,t} = c_{l,t}/v$, the cone angle for fast particles ($v \gg c_l$) being close to $\pi/2$. The slowing down of the particle (finiteness of the trajectory) smears out the cone to some extent, the smearing being dependent on the frequency: it is the greater the lower is the frequency. At extremely low frequencies ($c_l/\omega \gg L$, L is the particle track length) the radiation is not like the Cherenkov one at all. It is determined by the particle average acceleration and is similar to bremsstrahlung.

The Cherenkov mechanism of sound generation contributes appreciably to the sound field emitted by a particle only at very high hypersound frequencies (the spectral density of emitted energy is proportional to the third power of the frequency). So, according to Ref. 79, for the practically important frequency band of hundreds of kilohertz the ratio of the acoustic energy emitted by particles due to the Cherenkov mechanism of sound generation to the acoustical energy which is due to dynamic and thermoradiation mechanisms is 10^{-13} and 10^{-21}.

In concluding this part we note that just as transition radiation associated with motion of a charged particle through media with different electromagnetic properties exists in electrodynamics, so transition radiation-acoustic radiation may exist associated with change in radiation and acoustic properties of a medium in which the penetrating radiation is absorbed.[80] This transition radiation is relatively weak as is the Cherenkov one.

Sound generation mechanisms exist which are specific for this or that kind of penetrating radiation or of target substance. Let us dwell briefly on some of them.

4.6. Striction sound generation

Microstriction takes place in the field of ions in the course of ionization. It manifests itself appreciably in macroscopic effects.[81]

A moving charged particle (or any other moving parti-

cle capable of producing ionization) creates $N_1(0)$ ion pairs per unit track length in a medium. The number of these ions $N_1(t)$ decreases abruptly in time due to their recombination. Each ion will attract molecules of the medium by its field creating local compressed regions. The medium volume alterations per unit track length $\Delta V_1(t) = N_1(t)\Delta v$, where Δv is the medium volume alteration in the field of each ion (e.g. for water $\Delta v = 10^{-12}\text{cm}^3$). Let us determine now the change of $N_1(t)$ with time. Assuming that $N_1^0(t) \approx -\alpha N_1^2(t)/\pi r_{\text{tr}}^2$, where r_{tr} is the track "radius" (the distance to which electrons diffuse for slowing down and attachment) and α is the ion-ion recombination coefficient. Therefore

$$N_1(t) = N_1(0)/[1 + (t/t_0)], \quad t_0 = \pi r_{\text{tr}}^2/\alpha N_1(0).$$

The microstriction compression can play a considerable role in sound generation by charged particles under the conditions when the value of the thermal expansion coefficient of the medium is small. In particular, the results of the experiments of Refs. 30, 51 in which it was discovered that the sound pulse from a beam of charged particles in water becomes zero and changes its sign not at $T = 4\,^\circ\text{C}$ when the thermal expansion coefficient of water is $\beta = 0$, but at $T = 5.7\,^\circ\text{C}$ when $\beta = 10^{-5}\,(^\circ\text{C})^{-1}$ (see Fig. 16 and Fig. 17), is associated with the described microstriction effect. The pulse amplitudes become equal at $\beta = 10^{-5}\,(^\circ\text{C})^{-1}$, i.e. compensation of thermal expansion by striction compression is possible under these conditions.

Fast-oscillating striction exists also in the field of a moving particle and in the collective field of the beams besides the microelectrostriction in the field of the ions. Let us consider the striction mechanism of sound generation using the example of sound generation by laser radiation in a liquid.[82] The equation of sound generation by laser radiation in a liquid taking account of thermal and striction mechanisms takes on the following form:[82]

$$\Delta p - \frac{1}{c^2}\frac{\partial^2 p}{\partial t^2} = -\frac{\beta}{C_p}\frac{\partial Q}{\partial t} + \frac{1}{8\pi}\left(\rho\frac{\partial \varepsilon}{\partial \rho}\right)_T \Delta\langle E^2\rangle; \qquad (35)$$

here ε is the permittivity of the liquid, E is the electric field strength light in the liquid, $\langle \ldots \rangle$ denotes averaging over the period of light oscillations, $(\partial\varepsilon/\partial\rho)_T$ is the derivative of the permittivity with respect to the density at constant temperature. The second term on the right-hand side of equation (35) corresponds to the striction mechanism of sound generation. We cite the order-of-magnitude estimate[82] of the expression for $\Delta\langle E^2\rangle$:

$$\Delta\langle E^2\rangle \sim \left(\frac{1}{a^2} + k^2 + \mu^2\right)E_0^2 \sim \frac{8\pi}{nu}q_0\frac{1 + (ak)^2 + (a\mu)^2}{a^2},$$

where $n = \sqrt{\varepsilon}$ is the index of refraction of the medium, k is the wave number of the excited sound wave, a is the laser beam radius, μ is the light absorption coefficient in the liquid, E_0 is the electric field strength, u is the light velocity, q_0 is the light pulse intensity at the beam center. Since $|\partial Q/\partial t| \sim \mu q_0 \omega$ then the ratio of the first term on the right-hand side of equation (35) (describing the sources of the thermoradiation mechanism of sound generation) to the second term is equal to

$$\beta a n u \omega \left[C_p\left(\rho\frac{\partial\varepsilon}{\partial\rho}\right)_T \frac{\mu a}{1 + (a\mu)^2 + (a\mu)^2}\right]^{-1}$$

It follows from this ratio that the electrostriction mechanism of sound generation dominates over the thermoradiation one in only the region of very high or very low frequencies. For example, for water at $\mu \geqslant 0.2\ \text{cm}^{-1}$ in the frequency range from 10^2 to 10^9 Hz the thermoradiation mechanism will be dominant relative to the electrostriction one.

4.7. Other mechanisms of sound excitation by penetrating radiation

From among other mechanisms of sound generation by penetrating radiation we note the mechanism of excitation of elastic waves by the inverse piezoelectric effect[83] which is due to the mechanical deformation of a piezoceramic under the action of the electric field of penetrating radiation, and also the transition sound generation mechanism mentioned earlier.[80] Let us point out also that if a weakly ionized plasma is created in a region of the medium where penetrating radiation is absorbed, then the interaction of the electric and magnetic fields of the radiation with the plasma can lead to a disruption of the equilibrium state of the medium and, therefore, to emission of sound waves.

Sound generation mechanisms considered above have various physical limitations on the intensity, nature and frequency range of emitted sound waves. Numerical values can be obtained by the solution of concrete boundary-value problems. It is essential in this case that many sound generation mechanisms that were considered, contribute only small corrections to the sound field caused by the thermoradiation mechanism action in the majority of situations actually met in practice.

This is true only for the cases when the volume density of penetrating radiation energy evolved in a medium is small and there are no phase transitions.

The mechanisms, some of which were considered above, and also some specific nonlinear mechanisms similar to those existing due to laser radiation action, develop when the evolved energy density is large.[82,84,85] These mechanisms will not be considered here, however.

5. APPLICATIONS OF RADIATION ACOUSTICS

Some applications of radiation acoustics have already been dealt with in the literature (see, for example, the monograph of Ref. 12). We shall give here only the examples concerning the production quality control (radiation-acoustic microscopy and visualization), detection of super-high-energy elementary particles and an absolutely unusual, as it might seem, application of new generations of super-powerful accelerators in geoacoustics.

5.1. Scanning radiation-acoustic microscopy and visualization

The traditional methods of investigation and visualization of micro-objects, such as optical and electron microscopy, have many limitations. For example, optical and scanning electron microscopes have high resolution but they are useless for investigation of the inner regions of opaque objects. Difficulties arise in using x-ray TV microscopes associated with the deciphering of the obtained images, especially in the case of investigation of weak contrast objects.

There are no such shortcomings in the radiation-acoustic microscope (RAM).[21,22] The RAM operation principle is based on the effect of excitation and propagation of sound

and thermal waves in an object due to probing intensity-modulated penetrating radiation. We note that in the majority of cases the role of thermal waves is ignored as the dimensions of the region of heat evolution are always large compared with a thermal wavelength. On the contrary, in the case of RAM a penetrating radiation beam is focused, the region dimensions are small and thermal waves frequently play a fundamental role. Acoustic oscillations and thermal waves arising in an object are most frequently registered by sound sensors. The acoustic signal depends on the local properties of the object. Therefore, if the radiation beam moves in two mutually orthogonal directions, a radiation-acoustic image of the object is formed. In a general case it is the result of three processes: the variation in the absorbed power of the penetrating radiation due to the variation in the radiation properties of the object from one point to another, the interaction of the thermal waves with the thermal inhomogeneities of the object, and the interaction of acoustic waves with the elastic inhomogeneities of the object.

The first process carries information only on the radiation absorbtion properties of the object. If this process dominates then the radiation-acoustic image is essentially identical to the optical or scanned electron image. The RAM resolution in this case is determined by the diameter of the probing beam, and a subsurface structure visualization depth is determined by the depth of the radiation penetration. The second process is characterized by the interaction of thermal waves with the microinhomogeneities of the object. It gives qualitatively new information and allows one to expand significantly one's ideas concerning the physical properties of the object. The third process carries information on the mechanical irregularities of the object and plays an essential role if the acoustic wavelength is of the same order as the dimensions of the inhomogeneities in the object (usually this occurs at the intensity-modulation frequencies of the penetration radiation greater than 100 MHz). In this case the radiation-acoustic image is identical to the acoustic one (as in the acoustic microscope) and the resolution is of the order of a sound (hypersound) wavelength.

5.1.1. Scanning laser-acoustic (photoacoustic) microscopy

The historically first example of the radiation-acoustic microscopy was the laser-acoustic or, as it is frequently called, photoacoustic microscopy (PAM) (see, for example, Ref. 16 and also the review of Ref. 20 and the literature cited therein).

The photoacoustic microscope operation principle reduces to the following. A laser beam (in the IR, visible or UV range) intensity-modulated at the sound frequency moves along the surface of the irradiated object. The modulation is performed mechanically or electrically. An acoustic signal from the receiver goes to a synchronous detector via a preamplifier. The synchronous detector output is connected to a visualization device (a monitor, plotter or oscillograph with memory) with scans synchronized with the laser beam movement.

Depending on the method of recording the acoustic signal PAM is divided into schemes with a microphone (gas-microphone registration) and schemes with a piezotransducer. There are also PAM schemes with the acoustic signal registration by an auxiliary laser beam and photodetector.

Among the fields of application of PAM we single out nondestructive profile analysis—the investigation of the structure of layered inhomogeneous materials, integrated circuits testing, testing the chemical composition of complex compounds, investigation of changes in the crystal structure of semiconductors due to ion implantation, the possibility of visualization of volume or surface regions with different thermal characteristics caused by crystal structure inhomogeneities, a direct control of laser annealing, investigation of phase transitions in crystals and also measurements of thickness and control the uniformity of anode deposition of films on semiconductor substrates. Great expectations of PAM designers are associated with its application not only in the electronic industry but also in medicine and biology.

PAM is inferior in its resolution to optical and electron microscopes but it is superior to them in information content of images as it allows one to visualize the microstructure details of objects opaque to photons and electrons. This opens up new opportunities in microscopy and can expand and add to the traditional methods of microscopic analysis.

5.1.2. Scanning electron-acoustic microscopy (SEAM)

RAM schemes with electron excitation where the role of the laser beam is now played by an electron beam have been under development during the last decade and are applied already. A focused electron beam is used for the excitation of acoustic and thermal waves in a (solid) sample and acoustic signals are registered by a piezotransducer which is in direct contact with the sample. In other words, the same scheme is used as in PAM with a piezoreceiver. The first papers[17,18] describing electron-acoustic microscopy appeared about ten years ago (in 1980). The advantage of using electrons instead of photons is first of all in that the electron beam can be focused to a spot of smaller dimensions. Secondly, the electron track length depends on the electron energy and can be considerably greater in substances opaque to light than the range for photons. Both these factors open up opportunities for an increase in microscope resolution.

The first SEAM were designed on the basis of standard electron microscopes (SEM) and in fact represented a variant of their modernization. Essentially, the standard SEM is merely supplemented by several devices: an electron beam intensity modulator (additional deflection plates in the SEM chamber) and a sample holder in the SEM which is provided with a piezoreceiver with the necessary electronics for the amplification and visualization of the acoustic signal.

The SEAM turns out to be a more universal device than a standard SEM or even a scanning photoacoustic microscope (SPAM). Besides, one and the same device can, as a rule, operate in both regimes: i.e. SEAM and SEM. A comparison of images obtained in different operation modes opens up new opportunities in studies of the structure of a sample object under investigation.

Scanning electron-acoustic microscopy and visualization are used in microelectronics for quality control of integrated circuits, control of defects in the crystal structure of metals and alloys, investigation of the nature of dislocations and other disruptions of characteristics of materials under conditions of plastic deformations under large loads, visualization of the form of oscillations of a vibrating surface, and also for nondestructive testing for cracks in microsamples, parts, etc.

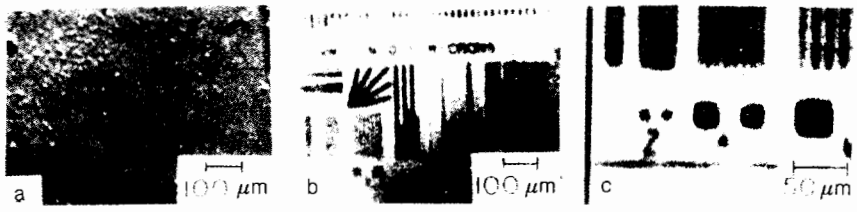

FIG. 34. The image of a silicon structure obtained with the help of SEM (a) and SEAM with different resolution (b and c).[19]

Figure 34 shows the images of a silicon structure with a phosphorescent coating as an illustration of SEAM capabilities. One can see that on the image (see Fig. 34a) obtained with the help of a standard scanning electron microscope (SEM), silicon structures are not visible under the coating. In contrast, Figs. 34b and c demonstrate a good quality image of a silicon structure obtained with the help of SEAM.

5.1.3. X-ray acoustic scanning visualization

Proposals to use an x-ray beam in scanning photoacoustic microscopy and visualization instead of a laser beam were discussed in Refs. 47, 48. The results of experimental studies of the scanning x-ray acoustic visualization were described in the paper of Ref. 49 which appeared not so long ago. The authors used synchrotron radiation in the x-ray range with an energy of 10 keV. The source was the high-energy synchrotron source of Cornell University (USA). The x-rays represented a periodic sequence of pulses with duration of 0.160 ns, an energy of 1.12 μJ per pulse and a repetition frequency of 360.6 kHz. The research was conducted using aluminum sample discs with a diameter of 5.72 cm and thickness of 1.52 cm. We note that the track length of x-ray quanta of an energy of 10 keV is 0.14 mm in aluminum. We indicate for comparison that for laser radiation it is equal to 3.76 nm.

A series of experiments was conducted using beam scanning in mutually perpendicular directions over the sample surface. The beam dimensions on the sample surface were 2×2 mm and the dimensions of the scanned area were 12×12 mm or 18×18 mm oriented according to the disc center.

The acoustic signal was received by a piezotransducer made of PZT-ceramic. Receivers with diameter of 18.5 and 1.3 mm were used. They were fixed at the center of the disc side opposite to the irradiated one. Experiments were conducted also when the receiver with a diameter of 1.3 mm was fixed on the lateral side of a disc. The receivers were damped in order to provide the necessary frequency range.

The research was conducted in two modes. In the one of them the collimated beam of x rays acted directly on the surface of a sample disc and moved in mutually perpendicular directions. The root mean square value of an acoustic signal amplitude was registered at the receiver-amplifier output. This value was presented on a video-monitor synchronously with the beam movement. The authors called another mode by the name of a double-modulation mode. This mode differed from the first one by the fact that the low-frequency intensity modulation of x rays was realized which, as it has already been mentioned, represented a periodic sequence of pulses with a very high repetition frequency (two–three orders higher than the modulation one) equal to 390.6 kHz. The use of the double modulation mode was based on the idea that a thermal wavelength in a sample target corresponding to the low-frequency envelope is greater than the one for the repetition frequency of the pulse sequence of the primary x rays. This allows one to increase the depth of the controlled (by a thermal wave) subsurface layer of the sample. The last statement turns out to be important as the acoustic waves of the megahertz range are attenuated rather fast.

One of the main problems which the authors of the experiments of Ref. 49 tried to solve, was to clear up the possibility of controlling defects by the x-ray acoustic method. This was the goal of the experiments on the visualization of a spatial picture of acoustic signal amplitude distribution excited by the x ray beam in a sample disc with an inner inhomogeneity in the form of a cylindrical cavity with the axis oriented in the plane of the disc. Measurements conducted both under the conditions without the low-frequency modulation of x rays and in the double-modulation mode have not allowed one to obtain a satisfactory image of the defect-cavity in the picture of the spatial distribution of the amplitudes of the acoustic signal excited in the disc by x rays. It was suggested in this connection to use the ratio of the root mean square values of the acoustic signal amplitudes for low-frequency envelopes in the target at two modulation frequencies as the information-carrying signal. Experimental results are given in Figs. 35a and b. They show the spatial distribution of the ratio of the root mean square amplitudes of the acoustic signals for the envelopes at frequencies 2.5/0.5 kHz and 1.5/0.5 kHz respectively. One can see quite an accurate image of the defect, i.e. a cylindrical cavity inside the sample disc. The conducted experiments confirmed a real opportunity to use x ray acoustic visualization for nondestructive testing. It is evident that under the conditions of sufficient focusing of an x-ray beam there is a real opportunity to realize scanning x-ray acoustic microscopy.

5.1.4. Ion-acoustic microscopy and visualization

The use of an ion beam for scanning radiation acoustic microscopy and visualization was discussed apparently for the first time in our reports in 1983.[21,22] In 1985 information about the construction of an ion-acoustic microscope appeared.[86] The results of the experimental research of the scanning ion-acoustic visualization of defects in metals was discussed recently in Ref. 87. In this research an ion beam was formed with the help of the modified beam optics of a standard ion mass-spectrometer. It was directed unto and moved upon the surface of an aluminum sample. The beam spot diameter on the sample surface was 300 nm. The acceleration voltage was varied in the range from 1 to 10 kV and the beam intensity modulation frequency was varied from 15 Hz to 20 kHz. The experiments had two goals. First, it was

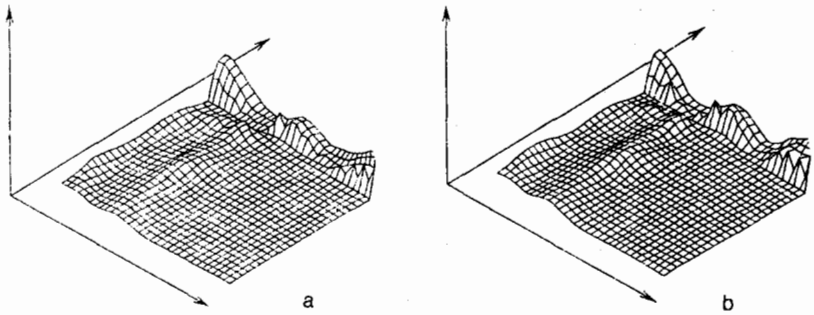

FIG. 35. The spatial picture of the distribution of the ratios root mean square amplitudes of acoustic signals for the envelopes at frequencies of 2.5/0.5 kHz (a) and 1.5/0.5 kHz (b).[49]

necessary to establish experimentally the character of the radiation-acoustic conversion and, second, to establish the possibility of applying it in the ion-acoustic visualization.

It was established experimentally that the dominant mechanism of sound excitation by a modulated ion beam due to its interaction with a substance in the examined ion energy range is the thermoradiation mechanism. It was shown also that an ion beam can be used effectively for scanning radiation-acoustic microscopy and visualization on an equal basis with photon beams (laser beam), electron beams and x rays.

5.2. Acoustic detection of super-high-energy particles in cosmic rays. The DUMAND project

The energy of 10^{17} eV (10^5 TeV) is accepted to be considered as the super-high-energy range in cosmic rays. The range boundary is not associated with some physical phenomenon, but is determined by the registration threshold of the extended atmospheric showers (EAS) resulting from the interaction of a high-energy particle with the atomic nuclei of matter in the atmosphere. The registration can be performed by the largest existing installations such as in Yakutsk (USSR), Haverah–Park (Great Britain) and others. The areas of these two installations are 18 and 12 square kilometers respectively. The installation dimensions are determined by the particle energy since the EAS dimensions increase with increasing energy and with the necessity to detect very rare events, i.e. the appearance of super-high-energy particles in the cosmic rays spectrum. The following data can give an idea of the number of registered events. There were registered 70,000 showers with an energy higher than $6\cdot10^{16}$ eV, 52,000 showers within the energy range of 10^{17}–10^{18} eV, 4,000 showers with an energy higher than 10^{18} eV, 144 showers with an energy higher than 10^{19} eV and only 16 showers with an energy of $5\cdot10^{19}$ eV during the ten years of the Haverah–Park installation operation.[88]

Astrophysicists are very interested in neutrino radiation. This interest is provoked first of all by the great penetration capability of neutrinos. A real opportunity to "look" into star bowels arise due to it. Neutrinos of super-high energy can provide information on high-energy processes taking place in the epoch of great red shifts and on unique physical objects such as hidden sources, etc.

A new branch has appeared in astrophysics—neutrino astronomy which has entered the stage of its experimental development. The Baksan neutrino telescope has been brought into operation in the Northern Caucasus. Similar installations are under construction abroad. However, the principal installation that may open up wide opportunities for experimental neutrino astronomy is DUMAND (Deep Underwater Muon and Neutrino Detector) when it will be brought into operation. This installation is as yet still in the design stage. We shall consider the DUMAND project further below.

Neutrino radiation is conventionally divided into two classes: atmospheric and cosmic neutrino radiation. In the first case neutrinos are generated as a result of interaction of accelerated particles with atomic nuclei of matter in the atmosphere. Cosmic neutrino radiation arises in space objects as a result of collision of accelerated particles with atomic nuclei and also due to the interaction of high energy protons with low-energy relict photons in space. High energy neutrinos are registered by secondary muons, hadrons and electrons produced by them due to the interaction of neutrinos with nucleons. In underground experiments muons are registered with the help of special detectors that are most frequently scintillation detectors. In underwater experiments the detector is water itself. Bremsstrahlung photons, electron-positron pairs and hadrons giving rise to electromagnetic and nuclear-elctromagnetic showers are born along a muon trajectory. At an energy > 100 TeV an electromagnetic shower beam arises along a muon trajectory. Hadrons generated in neutrino-nucleon collisions give rise to nuclear-electromagnetic showers. The length of such a shower in water or ground is small in contrast to an electromagnetic shower generated by a muon. This is why the showers caused by a neutrino can be recorded only if it interacted with nucleons inside the detector. In water the electrons of electromagnetic and nuclear-electromagnetic showers create the Cherenkov optical radiation which can be registered by a system of optical detectors, i.e. a lattice of photoreceivers.

The idea of the possibility of recording cosmic neutrinos was first suggested by Academician M. A. Markov in 1960.[89] A new stage of high-energy neutrino astronomy began with the discussion of the project of the deep underwater experiment DUMAND. Initially the DUMAND detector was planned to be a huge spatial lattice of photodetectors (1 km$\times$1 km$\times$1 km) submerged in the ocean at a depth of about 5 km. The distance between the sensitive elements (photodetectors) should not exceed the optical transparency length of water for visible and near-ultraviolet parts of the spectrum. The water layer over the installation serves as a shield from cosmic-ray muons.

G. A. Askar'yan and I. V. Dolgoshein[24,25] and independently Bowen[26,27] have suggested the acoustic method of recording super-high-energy neutrinos ($E_\nu > 10^7$ TeV).

This method is based on acoustic detection of particles proposed by G. A. Askaryan already in 1957.[7] It was suggested to replace the lattice of optical detectors by a cheaper lattice of acoustic detectors (hydrophones), especially, as there can be significantly fewer hydrophones than photodetectors in the lattice since the acoustic transparency of water is greater than its optical transparency.

The essence of the high-energy neutrino acoustic registration method consists of the following. A nuclear-electromagnetic cascade produced by the interaction of a neutrino with the detector substance is accompanied by a fast (practically instantaneous) heating of water in a narrow channel along the cascade axis. This causes the expansion of a volume of liquid in the channel and leads to the rise of a pressure pulse propagating in water at right angles to the cascade (shower) axis.

As estimates show, at a very high energy a narrow (several centimeters) and long ($L \approx 10$ m) beam of particles forms in the vicinity of the shower axis. Heating of the medium within the region of action of the beam occurs due to ionization losses of the shower electrons slowed down to an energy lower than the critical one. Therefore, a cylindrical thermoradiation sound source forms in the region of absorption of the shower electrons. Its radius (the radius of the heated part of the channel) is determined by the electron distribution over the channel cross section. The length is

$$L = \left(\ln \frac{E_h}{E_{cr}}\right)^{1/2},$$

where E_h is the shower energy (the energy of hadrons initiating the shower), $E_{cr} = 73$ MeV is the electron critical energy, L is in meters.

The authors of a large series of papers devoted to registration of high energy particles (to the DUMAND project) analyze the parameters of the sound field in the near wave zone of an electromagnetic cascade arising in water, i.e. of the thermoradiation source of sound.[24–27,90] They obtain the radiation-acoustic pulse form and amplitude using the equation of thermoradiation sound generation in a liquid and calculating the energy release function Q by different methods. The time dependence of the function $Q(r,t)$ is always taken in the form of a $\delta(t)$-function as the electromagnetic cascade rise time is much less than other characteristic "acoustic" times, while the spatial dependence is determined on the basis of some approximations and different direct calculations of the energy release density in the cascade. For example, the following expression for the calculation of a radiation-acoustic signal amplitude in sea water is given in Ref. 91

$$p_{max} = \frac{0{,}44\varphi(r)E_h}{\sqrt{r}E_0},$$

where p_{max} is the sound pressure (in Pa), E_h is the particle energy (in eV), $E_0 = 10^{18}$ eV, r is the distance from the channel axis (in meters). The factor $\varphi(r)$ takes into account the deviation of a sound signal attenuation law from the cylindrical one ($r^{-1/2}$) and $\varphi(r) = 1.0$; 0.95; 0.28; 0.12 for $r = 50$, 100, 250 and 500 m respectively. The acoustic signal amplitude for a particle with an energy $E_h = 10^{17}$ eV at a distance of 100 m from the cascade axis is equal to $p_{max} = 4 \cdot 10^{-3}$ Pa. The acoustic signal form and its maximum amplitude will in fact depend on the special features of ionization losses in the nuclear-electromagnetic shower channel, i.e. on the form of the distribution function describing the energy release, $Q(r,t)$.

In order to detect the acoustic signal from a shower in the ocean it is important to know not only the signal amplitude and form (its spectrum) but also the value of sound attenuation during its propagation as well as interference characteristics, i.e. the spectrum of environmental noise in the ocean. All this leads to the necessity of determination of the optimal detection frequency band of the radiation-acoustic signal. The sound attenuation decreases as the frequency decreases (i.e. the sound absorption length increases) but, on the other hand, it is known that the environmental noise level (interference) in the ocean increases as the frequency decreases. That is why in the majority of papers associated in one way or another with the DUMAND project the estimates of the effective sound pressure value are given either for some optimal frequency band or at a fixed (optimal) frequency.

5.3. Neutrino for geoacoustics. The GENIUS project

The possible use of high-energy neutrino beams in geophysics and, in particular, in geoacoustics can serve as an example of the future applications of new generations of powerful accelerators. The neutrinos can play here, figuratively speaking, the same role as that of x rays in medicine and in nondestructive testing.

A rough scheme of applications of neutrino beams in geophysics is as follows.[30,31] A neutrino beam formed by an accelerator is aimed in a specified direction and travels over a considerable distance (hundreds and thousands of kilometers) in the Earth. As it propagates the beam generates secondary radiation of different types: muon, radio and acoustic.

Neutrinos themselves can be a probing device: neutrino absorption along its path can be a measure of the quantity of matter along it. Secondary radiation beams in this case serve for neutrino beam detection and measurement of its parameters. In other cases a neutrino beam can be used only as a source of secondary radiation which in the course of propagating "selects" information on the characteristics of the Earth. The realization of geoacoustic (as well as geophysical) applications of neutrino beams demands contradictory conditions to be satisfied: neutrino penetrating capability must be combined with a strong interaction with matter, as the neutrino beam must perform the role of a powerful thermoradiation sound source. As calculations showed, these conditions can be satisfied for the neutrino beams of an energy > 10 TeV and higher. A neutrino beam of such energy produced by an accelerator is narrow and sharply directed, and this provides the high volume density of the energy released due to its interaction with matter. This creates the conditions of efficient sound generation in ground or water.

Thus, when we speak about neutrinos for geoacoustics, we speak, certainly, about ideas that as yet are only fantastic and at present we can speak only about projects and forecasts for the accelerators of future generations. Moreover, the phenomena taking place at such an energy can be observed now only in experiments with cosmic rays (they were considered in the preceding section) and to a large extent they need further investigation.

A. Rujula, S. Glashow, R. Wilson and R. Charpak,[30] who introduced the idea of using a thermoacoustic signal generated in rocks by a neutrino beam for geological research, were apparently the first who made estimates of proton accelerator parameters needed for the creation of the required neutrino beam and the acoustic signal generated by it. On these estimates they based their proposal for the GENIUS (Geological Exploration Neutrino Induced Underground Sound) project. They considered the possibility of construction of a circular accelerator for a proton energy of $E_p = 3$–20 TeV which was named "Geotron" in contrast to the proton accelerator for an energy of $E_p \simeq 1$ TeV named "Tevatron" since in the latter case new generation accelerators for a teraelectronvolt energy are meant.

Thus, the GENIUS project can be a second example of an immense project in the field of high-energy physics and radiation acoustics. We can consider the DUMAND project to be the first.

While it is significant that a proton accelerator for an energy of $E_p = 1$ TeV will every few minutes "eject" 10^{14} protons with a total kinetic energy of 1 MJ, then these parameters are even more impressive for the "Geotron". Thus, for example, the number of protons per pulse is 10^{15} and total energy is $E = 10^9$ J. If one will use the most modern superconductors for the construction of the accelerator magnet system, the radius of its circular vacuum channel will be equal approximately to 6 km for a proton energy of $E_p = 10$ TeV and for a proton energy of $E_p = 20$ TeV it will correspondingly be 12 km. The synchrotron radiation power is a very important parameter of the accelerator. The authors of Ref. 32 estimate this power to be equal to 16 and 64 kW respectively. The authors of Ref. 30 consider as one of the possibilities the construction of the circular chamber of a proton accelerator for an energy of $E_p = 10$–20 TeV in the sea in order to protect nearby people from the synchrotron radiation.

A neutrino beam propagating deep in Earth is the source of acoustic waves in neutrino geoacoustic prospecting. The sound detection has to be conducted by a geophone array on the Earth surface or by a hydrophone array if the acoustic signal measurements are conducted in the sea.

Speaking about the neutrino beam parameters we must note that estimates show that for an accelerator for a proton energy of $E_p = 10$ TeV the neutrino beam diameter at a distance of 1000 km from the accelerator will be about 10 m and the neutrino flux in the beam will be 10^{10} neutrinos per square meter. The sound pressure amplitude at a distance of 1000 m from the beam axis is 10^{-5} Pa and the optimal frequency band lies in the region of $f \approx 100$ Hz.

The signal amplitude turns out to be very small. However, the value of the signal-to-noise ratio is the fundamental parameter from the point of view of signal detection. The noise level (seismic noise or ocean noise, if one considers underwater detection) in the characteristic frequency range ($f \sim 100$ Hz) can be approximately five orders higher than the signal level. Nevertheless, signal detection under these conditions can be not entirely hopeless. The noise stability can be increased by using a lattice-array with a large number of detectors. If the noise at the array detectors is uncorrelated and, conversely, the signal at all the detectors is correlated, then the noise stability of detection increases directly proportional to $\sqrt{n}$, where n is the number of detectors in the array. Moreover, one can use coherent signal storage to increase the detection noise stability since the sound source and the detection array position is fixed and the storage time can be chosen sufficiently great. In particular, the use of a linear pion accelerator instead of a circular proton accelerator in "Geotron" construction would be favorable for this. This would allow one to increase the repetition frequency of neutrino (geoacoustic) pulses.

6. CONCLUSION

We can first of all state that theoretical and experimental research on the thermoradiation mechanism of sound generation by penetrating radiation in condensed media is now quite advanced. The generation processes due to continuous (modulated) and pulsed action of penetrating radiation on a substance have been studied. Basic laws of acoustic signal formation have been established and the connection of the characteristics of these signals with the radiation parameters, as well as with the thermodynamic, acoustic and radiation properties of matter has been elucidated. The theory of thermoradiation sound generation in condensed media was confirmed convincingly by experiments. This provides an opportunity to make well-founded choices of penetrating radiation sources for the solution of practical problems, such as radiation-acoustic microscopy and visualization, application of radiation-acoustic effects in nondestructive testing, etc. Prospects are opening up of realizing immense and, may be, fantastic (from a modern point of view) projects in neutrino astrophysics (the DUMAND project) and neutrino geoacoustics (the GENIUS project). Radiation excitation of sound can be useful also in other situations which could seem unusual: for example, for acoustic signal excitation in cosmic bodies with the help of laser radiation from the Earth or penetrating radiation beams from space platforms, creation of vertical underwater radiating arrays with the effective height of several tens of meters in the ocean (if one will use laser radiation in the blue-green optical range) or extended arrays with a length of tens and hundreds of kilometers (with the help of neutrino beams). These are problems that do not have simple solutions using traditional radiators.

Summarizing, it must be emphasized, however, that practically in the entire article we considered the linear theory which, as could be seen, allows one to describe radiation-acoustic effects when the penetrating radiation intensity or, more precisely, the density of the penetrating radiation energy evolved in a medium is small. We considered the nonlinear mechanism of radiation sound generation for several cases only. This was done when we spoke about the radiation effects arising due to action of heavy particles, fission fragments and delta electrons, but generally speaking, the phenomenon of penetrating radiation interaction with matter is nonlinear by its nature. And from this point of view, both theory and experiment (practical applications of the conclusions of the linear theory) are limited to small perturbations (small intensities). Secondly, even within the framework of the linear theory only comparatively simple situations were considered. Speaking about thermoradiation sound generation in solids, we must admit that only the simplest model of an isotropic elastic body was considered. In practice one has

to deal with bodies of complex structure, such as semiconductors, piezoelectrics and ferroelectrics, ferromagnetics, etc., in which it is important to take into account the penetrating radiation interaction in a sound generation process with different subsystems: the lattice, electron-hole, spin and other subsystems as well as the interaction of these subsystems in complex solid state structures.

Wide prospects for creation of new technologies can be opened up by research on nonlinear radiation-acoustic effects. Nonlinear acoustic effects in a substance already arise even when there is no change in the aggregate state of the substance and no phase transitions, but when the rate of volume expansion of the substance absorbing the penetrating radiation is great enough. A region of the medium in this case serves as a source of waves of finite amplitude which, in their turn, can transform into shock waves. Mechanical, physical and chemical properties of a substance can change due to action of these shock waves. This fact can be used for new technologies. Self-induced oscillation processes can arise due to powerful penetrating radiation action on a substance when phase transitions take place.[92] Substance evaporation or, for example, an optical breakdown under the action of powerful laser radiation can take place and shock waves or sound waves of tremendous amplitude with parameters unattainable by traditional methods can arise.

Powerful radiation sources have been developed already or are under design. It is regrettable that frequently they are intended for use in ray and beam weapons as was indicated in the review published by american physicists.[93] Let us hope that these sources will never be used for the purpose for which they were designed, but will find an application for peaceful purposes including radiation acoustic technologies.

Notes added in proof:

1. Reports have appeared recently (see: U. Amaldi, W. de Boer and H. Furstenau, Phys. Lett. B **260**, 447 (1991); S. Dimopoulos, S. A. Raby and F. Wilczek, Phys. Today, **44** (10) 25 (1991) that the results of very precise measurements conducted recently support the predictions of the minimal supersymmetric SU (5) model that unifies electromagnetism and the weak and strong interactions. Such "unification" (if it exists) is expected to be observed at an energy $E \leqslant 10^{19}$ MeV.

2. Local heatings arising on particle tracks in dense stable media and giving rise to sound pulses and also bubbles generating hypersonic waves are considered in Refs. 7, 8 in contrast to Ref. 6 where the problem of sound emission due to appearance of bubbles on particle tracks in metastable media was discussed. Acoustic registration of particles is proposed in Refs. 7, 8. The possibility of appearance of hypersonic pulses in the process of radiobiological action of radiation on cells and chromosomes (as a part of destructive action) is noted.

3. Such an approximation is very imprecise even because the diameter (radius) of a nuclear-electron-photon cascade increases as the shower develops.

4. A report appeared (see: A. B. Borisov, A. V. Vasil'kov, A. E. Volotskiĭ *et al.*, Zh. Exp. Teor. Fiz. **100** 1121 (1991) [Sov. Phys. JETP **73**, 619 (1991)] when this review was already in print, on registration of an acoustic signal from the muon beam of the neutrino channel of the U-70 accelerator (High Energy Physics Institute). The authors studied the acoustic signals from the muon flux in the muon filter of the neutrino channel. The results of measurements of the signal and the theoretical estimates based on the thermoradiation generation mechanism are given. A satisfactory agreement between experimental and theoretical data is noted, and this is evidence of the dominant contribution of the thermoradiation mechanism. The possibilities of using the radiation-acoustic method for long-range determination of characteristics of particles beams at an accelerator are considered.

The author is deeply grateful to Yu. V. Gulyaev for the discussions which stimulated the writing of this article and to G. A. Askar'yan for useful remarks made during the preparation of the manuscript for publication.

[1] W. S. Roentgen, Philos. Mag. **11**, 308 (1881).
[2] A. G. Bell, *ibid.* **11**, 510 (1881).
[3] See: J. Tyndall, *Sound*, Longmans, Green, London, 1913 [Russ. transl. GIZ, M., 1922].
[4] M. I. Kaganov, I. M. Lifshits and L. V. Tanatarov, Zh. Eksp. Teor. Fiz. **31**, 232 (1956) [Sov. Phys. JETP **4**, 173 (1957)].
[5] M. J. Buckingham, Proc. Phys. Soc. London **66**, 601 (1953).
[6] D. A. Glaser and D. C. Rahm, Phys. Rev. **91**, 474 (1955).
[7] G. A. Askarian [in Russian], At. Energ. **3**, 152 (1957).
[8] G. A. Askarian, Zh. Tekh. Fiz. **29**, 267 (1959) [Sov. Phys. Tech. Fiz. **4**, 234 (1959)].
[9] R. M. White, J. Appl. Phys. **34**, 2123 (1963).
[10] R. A. Graham and R. E. Hutchison, Appl. Phys. Lett. **11**, 69 (1967).
[11] B. L. Beron and R. Hofstadter, Phys. Rev. Lett. **23**, 184 (1969).
[12] I. I. Zalyubovskiĭ, A. I. Kalinichenko, and V. T. Lazurik, *Introduction to Radiation Acoustics* [in Russian], Vishchya shkola, Kiev, 1986.
[13] L. M. Lyamshev and B. I. Chelnokov, Akust. Zh. **29**, 372 (1983) [Sov. Phys. Acoust. **29**, 220 (1983)].
[14] L. M. Lyamshev and B. I. Chelnokov, *Radiation Acoustics* [in Russian], (Ed.) L. M. Lyamshev, Nauka, M., 1987, p. 58.
[15] F. S. Perry, Appl Phys. Lett. **17**, 408 (1970).
[16] G. Busse and A. Rosencwaig, *ibid.* **36**, 815 (1980).
[17] E. Brundis and A. Rosencwaig, *ibid.* **37**, 98 (1980).
[18] G. Cargill, Nature **286**, 691 (1980).
[19] G. Cargill, Phys. Today **34**(10), 27 (1981).
[20] A. I. Morozov and V. Yu. Raevskiĭ [in Russian], Zarubezh. electron. tekhnika, 1982, No. 2, p. 46.
[21] L. M. Lyamshev and B. I. Chelnokov, Akust. Zh. **30**, 564 (1984) [Sov. Phys. Acoust. **30**, 334 (1984)].
[22] L. M. Lyamshev and B. I. Chelnokov [in Russian], Abstracts of the All-Union Conference "Interaction of ultrasound with biological media," N. N. Andreev Acoustical Institute of the Academy of Sciences of the USSR, Moscow, 1983, p. 65.
[23] V. S. Berezinskiĭ [in Russian], Priroda, 1976, No. 11, p. 28.
[24] G. A. Askar'yan and B. A. Dolgoshein [in Russian], Preprint No. 160, FIAN SSSR, Moscow, 1976.
[25] G. A. Askar'yan and B. A. Dolgoshein, Pis'ma Zh. Eksp. Teor. Fiz. **25**, 232 (1977) [JETP Lett. **25**, 213 (1977)].
[26] T. Bowen, Proc. 1976 DUMAND Summer Workshop, Honolulu, Sept. 6–19, Batavia, USA, FNAL, 1977, p. 523.
[27] T. Bowen, 15 Intern. Cosmic Ray Conference, Plovdiv, Bulgaria, 1977, Sofia, 1977, v. 6, p. 277.
[28] V. S. Berezinskiĭ and G. T. Zatsepin, Usp. Fiz. Nauk **122**, 3 (1977) [Sov. Phys. Usp. **20**, 361 (1977)].
[29] L. M. Lyamshev, A. V. Furduyev, B. I. Chelnokov and V. I. Yakovlev, Akust. Zh. **31**, 709 (1985) [Sov. Phys. Acoust. **31**, 435 (1985)].
[30] A. Rujula, S. Glashow, R. Wilson and G. Charpak, Prepr. HUTP-83/A019, Stanford, 1983.
[31] V. A. Tsarev and V. A. Chechin, *Neutrino for Geophysics* [in Russian], Znanie, M., 1985, (Fizika, No. 12).
[32] L. M. Lyamshev, J. Phys. (Paris) Colloq. **51**, C2, Suppl. Nr. 2, C2-1 (1990).
[33] L. M. Lyamshev and B. I. Chelnokov [in Russian], Ref. 14, p. 58.
[34] E. M. Segre, (Ed.) *Experimental Nuclear Physics*, Wiley, N. Y., 1953 [Russ. transl., IIL, M., 1955, v.1].
[35] L. S. Gournay, J. Acoust. Soc. Am. **40**, 1322 (1966).
[36] Chia-Lun Hu, *ibid.* **46**, 728 (1969).
[37] L. M. Lyamshev, *Laser Thermo-optical Excitation of Sound* [in Russian], Nauka, M., 1989.
[38] A. I. Bozhkov, F. V. Bunkin, A. A. Kolomenskiĭ, A. I. Malyarovskiĭ and V. G. Mikhalevich [in Russian], Trudy FIAN, 1984, v. 56, p. 123.

[39] L. M. Lyamshev and L. V. Sedov, Akust. Zh. **25**, 906 (1979) [Sov. Phys. Acoust. **25**, 510 (1979)].
[40] A. I. Bozhkov, F. V. Bunkin, A. A. Kolomenskiĭ *et al.*, Pis'ma Zh. Tekh. Fiz. **6**, 1313 (1980) [Sov. Tech. Phys. Lett. **6**, 563 (1980)].
[41] G. A. Askarijan, B. A. Dolgoshein, A. N. Kalinovsky and N. V. Mokhov, Nucl. Instrum. Methods **164**, 267 (1979).
[42] L. M. Lyamshev [in Russian], *Proceedings of XI All-Union Acoustic Conference, Invited Lectures*, AKIN AN SSSR, Moscow, 1977, p. 5.
[43] T. G. Muir, C. R. Culbertson and J. R. Clynch, J. Acoust. Soc. Am., **59**, 735 (1976).
[44] L. Hutcheson, O. Roth and F. Barnes, *Records of 11th Symp. on Electron, Ion and Laser Beams Technology*, Boulder, Col., 1971, p. 413.
[45] S. G. Kasoev and L. M. Lyamshev, Akust. Zh. **23**, 890 (1977) [Sov. Phys. Acoust. **23**, 510 (1977)].
[46] A. M. Aindow, R. J. Dewhurst, D. A. Hutchins and S. B. Palmer, J. Acoust. Soc. Am. **69**, 449 (1981).
[47] K. Y. Kim and W. Sachse, *Proc. 1983 IEEE Ultrasonics Symposium*, 1983, p. 677.
[48] K. Y. Kim and W. Sachse, Appl. Phys. Lett. **43**, 1099 (1983).
[49] W. Sachse, K. Y. Kim and V. P. Pierce, IEEE Trans. on Ultrason., Ferroelast. and Frequency Control UFFC-33, 546 (1986).
[50] I. A. Danil'chenko, I. E. Lbov *et al.* [in Russian], Ref. 14, p. 51.
[51] S. D. Hunter and V. W. Jones, J. Acoust. Soc. Am. **69**, 1557 (1981).
[52] L. R. Sulak, AIP Conf. Proc. No. 52 on Long-Distance Neutrino Detection, New York, 1979, p. 85.
[53] G. A. Askar'yan and B. A. Dolgoshein, Pis'ma Zh. Eksp. Teor. Fiz. **28**, 617 (1978) [JETP Lett. **28**, 571 (1978)].
[54] V. D. Volovik and G. F. Popov, Pis'ma Zh. Tekh. Fiz. **1**, 601 (1975) [Sov. Tech. Phys. Lett. **1**, 270 (1975)].
[55] P. I. Golubnichiĭ, G. S. Kalyuzhnyĭ, S. D. Korchikov *et al.*, *ibid.* **7**, 272 (1981) [*ibid.* **7**, 117 (1981)].
[56] P. I. Golubnichiĭ, G. S. Kalyuzhnyĭ, V. I. Nikol'skiĭ and V. I. Yakovlev, Kratk. Soobshch. Fiz. No. 9, 19 (1978) [Sov. Phys. Lebedev Inst. Rep. No. 9, 16 (1978)].
[57] L. Sulak, T. Armstrong, H. Baranger *et al.*, Nucl. Instrum. Methods **161**, 203 (1979).
[58] I. A. Borshkovskiĭ and V. D. Volovik, Izv. Vyssh. Uchebn. Zaved. Fiz. No. 10, 72 (1973) [Sov. Phys. J. **16**, 1398 (1973)].
[59] I. A. Borshkovskiĭ, V. D. Volovik, and V. T. Lazurik-El'tsufin [in Russian], Zh. Prikl. Mekh. Tekh. Fiz. No. 2, 138 (1975) [J. Appl. Mech. Tech. Phys. (1975)].
[60] I. A. Borshkovskiĭ, V. D. Volovik *et al.* Pis'ma Zh. Eksp. Teor. Fiz. **13**, 546 (1971) [JETP Lett. **13**, 390 (1971)].
[61] I. A. Borshkovskiĭ, V. D. Volovik, I. A. Grishaev *et al.*, Zh. Eksp. Teor. Fiz. **63**, 1337 (1972) [Sov. Phys. JETP **36**, 706 (1973)].
[62] V. A. Balitskiĭ, V. V. Bukreev, G. S. Kalyuzhnyĭ, and V. A. Tsarev [in Russian], Preprint FIAN, No. 138, Moscow, 1988.
[63] V. A. Balitskiĭ, V. S. Gorodetskiĭ, L. M. Lyamshev *et al.*, Akust. Zh. **31**, 694 (1985) [Sov. Phys. Acoust. **31**, 422 (1985)].
[64] D. I. Vaisburd, E. N. Semin *et al.*, *High Energy Electronics of Solids* [in Russian], Nauka, Siberian Branch of the Academy of Sciences of the USSR, Novosibirsk, 1982.
[65] V. I. Oleshko and N. F. Shtan'ko, Zh. Tekh. Fiz. **57**, 1857 (1987) [Sov. Phys. Tech. Phys. **32**, 1114 (1987)].
[66] V. A. Malugin and A. V. Manukin, Pis'ma Zh. Tekh. Fiz. **9**, 819 (1983) [Sov. Tech. Phys. Lett. **9**, 352 (1983)].
[67] D. Adlene, E. Pranevesins and A. Ragaiscas, Nucl. Instr. Methods **209–210**, 357 (1982).
[68] P. G. Satkewicz, J. S. Murphy *et al.*, *Reviews of Progress in Quantitative Nondestructive Evaluation*, Plenum, New York; London, 1986, No. 54, p. 455.
[69] V. I. Gol'danskiĭ, E. Ya. Lantsburg, and N. A. Yampol'skiĭ, Pis'ma Zh. Eksp. Teor. Fiz. **21**, 365 (1976) [JETP Lett. **21**, 166 (1975)].
[70] A. I. Anoshin, Zh. Tekh. Fiz. **47**, 2186 (1977) [Sov. Phys. Tech. Phys. **22**, 1270 (1977)].
[71] V. D. Volovik and G. F. Popov, Pis'ma Zh. Tekh Fiz. **1**, 601 (1975) [Sov. Tech. Phys. Lett. **1**, 270 (1975)].
[72] V. D. Volovik, V. V. Petrenko, and G. F. Popov, *ibid.* **3**, 459 (1977) [*ibid.* **3**, 185 (1977)].
[73] V. D. Volovik, A. I. Kalinichenko, V. T. Lazurik and G. F. Popov, Zh. Tekh. Fiz. **49**, 1343 (1979) [Sov. Phys. Tech. Fiz. **24**, 745 (1979)].
[74] P. Marietti, D. Sette and F. Wanderlingh, J. Acoust. Soc. Am. **45**, 515 (1969).
[75] P. I. Golubnichiĭ, V. G. Kudlenko, and V. I. Yakovlev, Akust. Zh. **31**, 703 (1985) [Sov. Phys. Acoust. **31**, 430 (1985)].
[76] I. A. Akhiezer and V. T. Lazurik-El'tsufin, Exp. Teor. Fiz. Zh. **63**, 1776 (1972) [Sov. Phys. JETP **36**, 939 (1972)].
[77] N. N. Nasonov [in Russian], Ukr. Fiz. Zh. **27**, 1957 (1982).
[78] I. M. Kaganova and M. I. Kaganov, Fiz. Tverd. Tela (Leningrad) **15**, 2119 (1973) [Sov. Phys. Solid State **15**, 1410 (1973)].
[79] I. A. Borshkovskiĭ and V. D. Volovik, Izv. Vyssh. Uchebn. Zaved. Fiz. No. 10 72 (1973) [Sov. Phys. J. **16**, 1398 (1973)].
[80] V. I. Pavlov and A. P. Sukhorukov, Usp. Fiz. Nauk **147**, 83 (1985) [Sov. Phys. Usp. **28**, 784 (1985)].
[81] G. A. Askar'yan and B. A. Dolgoshein, Pis'ma Zh. Eksp. Teor. Fiz. **28**, 617 (1978) [JETP Lett. **28**, 571 (1978)].
[82] F. V. Bunkin and M. I. Tribel'skiĭ, Usp. Fiz. Nauk **130**, 193 (1980) [Sov. Phys. Usp. **23**, 105 (1980)].
[83] V. D. Volovik and S. I. Ivanov, Zh. Tekh. Fiz. **45**, 1789 (1975) [Sov. Phys. Tech. Phys. **20**, 1140 (1975)].
[84] L. M. Lyamshev, Usp. Fiz. Nauk **135**, 637 (1981) [Sov. Phys. Usp. **24**, 977 (1981)].
[85] L. M. Lyamshev and K. A. Naugol-'nykh, Akust. Zh. **27**, 641 (1981) [Sov. Phys. Acoust. **27**, 357 (1981)].
[86] H. Tateno, T. Ono *et al., Proc. 6th Symposium on Ultrasonic Electronics*, Tokyo, 1985; Jpn. J. Appl. Phys., **25**, Suppl. 25-1, 188 (1986).
[87] P. G. Satkewicz, J. S. Murphy *et al.*, Ref. 68, p. 455.
[88] V. S. Berezinskiĭ, S. V. Bulanov, V. L. Ginzburg, (Ed.) *et al.*, *Astrophysics of Cosmic Rays*, North Holland, Amsterdam 1990 [Russ. original, Nauka, M., 1984].
[89] M. A. Markov, *Proc. 10th Intern. Conference on High-Energy Physics*, Rochester, England, 1960, p. 579.
[90] V. D. Volovik, A. I. Kalinichenko, V. T. Lazurik and G. F. Popov, Pis'ma Zh. Tekh. Fiz. **4**, 611 (1978) [Sov. Tech. Phys. Lett. **4**, 245 (1978)].
[91] G. A. Askarijan, B. A. Dolgoshein, A. N. Kalinovsky and N. V. Mokhov, Nucl. Instrum. Methods **164**, 267 (1979).
[92] S. V. Selischev, *Self-induced processes under the action of concentrated energy flows on materials* (In Russian) Dr. Sci. Thesis, Institute of Thermophysics of the Siberian Branch of the Academy of Sciences of the USSR, Novosibirsk, (1988).
[93] Report to the American Physical Society of the Study Group on Science and Technology of Directed Energy Weapons, Phys. Today **40**(5), S1 (May 1987) [Russ. transl., Usp. Fiz. Nauk **155**, 659 (1988).

English text provided by the author.